RNA-based boronate internucleosidic linkages: an entry into reversible templated ligation and loop formation

Alejandro Gimenez Molina, Ivan Barvik, Sabine Müller, Jean-Jacques Vasseur and Michael Smietana

ELECTRONIC SUPPLEMENTARY INFORMATION

CONTENT

List of Tables and Figures

Pages

General

All reagents were purchased from local suppliers and used without purification. All unmodified oligonucleotides used for this study were purchased from Eurogentec. Synthesized 5' borono-oligoribonucleotides (U^{bn}) and 5´-borono-oligonucleotides (T^{bn}) were purified by RP-HPLC (Dionex Ultimate 3000) with a Nucleodur 100-7 C18 column (125 x 8 mm; Macherey-Nagel) and analyzed with a Accucore aQ column (50 x 4.6 mm; Thermo Scientificl) and by MALDI-TOF MS (Voyager PerSeptive Biosystems) using trihydroxyacetophenone (THAP) as matrix and ammonium citrate as co-matrix. Thermal denaturation experiments were performed on a VARIAN Cary 300 UV spectrophotometer equipped with a Peltier temperature controller and a thermal analysis software.

Chemical Synthesis

2´-*O*-PivOM-3´-*O*-TBDMS-5´-*O*-DMTr Uridine (2)

Commercially available 2´-*O*-Pivaloyloxymethyl-5´-*O*-(4,4´-Dimethoxytrityl) Uridine (**compound 1**) (2.89g, 4.37mmol) and Imidazole (1.19g, 17.48mmol) were co-evaporated in dry pyridine (3 x 90mL) and dissolved in 90mL of dry pyridine. To the mixture was added dropwise and under Argon atmosphere, a solution of *tert*-butyldimethylsilyl chloride (1.31g, 8.74mmol) in 30mL of dry pyridine. The mixture was stirred at r.t. for overnight. The reaction was quenched by the addition of 9mL of water, diluted in 45mL of ethyl acetate and followed by extractive work-up with aq. $NaHCO_3$ (2 x 15mL). The aqueous phase was back-extracted with more ethyl acetate (2 x 45mL), the organic phases dried over Na_2SO_4, filtered, evaporated to oil and co-evaporated in heptane (3 x 50mL). The residue was purified by silica gel column chromatography using a gradient of 1-3% MeOH in dichloromethane containing 1% Et_3N to afford **compound 2** in 97% yield (3.28g, 4.23mmol). ^{1}H-NMR (300MHz, CD_3CN): δ 7.83 (d, $J_{H\text{-}6/H\text{-}5}$ = 8.1Hz, 1H, H6); 7.45-7.24 (m, 9H, Har, DMTr); 6.89-6.86 (m, 4H, Har, DMTr); 5.92 (d, $J_{H1'\text{-}H2'}$=3.1Hz, 1H, H1´); 5.46, 5.29 (2d_{AB}, J_{AB} = 6.4Hz, 2H, OCH_2O, PivOM); 5.37 (d, $J_{H5\text{-}/H6}$ =8.1Hz, 1H, H5); 5.35 (m, 2H, H3´and H2´); 4.04 (m, 1H, H4´); 3.75 (s, 6H, 2 OCH_3); 3.54 (dd, $^2J_{H5'/H5''}$ =11.1Hz, $^3J_{H5'/H4'}$ =2.6Hz, 1H, H5´); 3.32 (dd, $^2J_{H5'/H5''}$ =11.1Hz, $^3J_{H5'/H4'}$ =3.3Hz, 1H, H5´´); 1.15 (s, 9H, $OCOC(CH_3)_3$, PivOM); 0.80 (s, 9H, $OSiC(CH_3)_3$, TBDMS); 0.06, -0.02 (2x s,6H, $Si(CH_3)_2$, TBDMS). ^{13}C-NMR (75MHz, CD_3CN): δ 178.4 (OC=O); 164.1 (C=O); 159.8; 151.3 (C=O); 145.5; 141.3; 136.3 (Cq, Ar); 136.2 (C6); 131.1; 129.0; 128.9; 128.0; 114.1 (CH, Ar); 102.7 (C5); 89.2 (C1´); 88.6 (OCH_2O, PivOM); 87.7 (CH, Ar); 84.3 (C4´); 81.7 (C2´); 71.0 (C3´); 63.0 (C5´); 55.9 (OCH_3, DMTr); 39.4 ($OCOC(CH_3)_3$, Cq, PivOM); 27.2 ($OCOC(CH_3)_3$, PivOM); 26.0 ($OSiC(CH_3)_3$, TBDMS); 18.5 ($SiC(CH_3)_3$, Cq, TBDMS); -4.2, -4.7 (2x $SiC(CH_3)_2$). HRMS (ESI) Calcd for $C_{42}H_{54}N_2O_{10}Si$ $[M\text{-}H]^-$ 773.3106; found, 773.3148.

2´-*O*-PivOM-3´-*O*-TBDMS Uridine (3)

Compound 2 (2.32g, 2.99mmol) was dissolved in a 7:3 mixture (v/v) of dichloromethane and MeOH (40mL). A solution of 10% benzene sulfonic acid (w/v) in dichloromethane/MeOH 7:3 (13.4mL) was added dropwise to the reaction mixture in an ice-bath, and stirred for 30min at 0ºC. The orange solution was allowed to stand for another 25min at rt., washed with saturated aq. $NaHCO_3$ (100mL) and the organic phase dried over Na_2SO_4. Purification by column chromatography on silica gel using a gradient of 0-60% EtOAc in Cyclohexane gave **compound 3** in 93% yield as a white solid material (1.31g, 2.77mmol). ^{1}H-NMR (400MHz, $CDCl_3$): δ 8.84 (b.s, 1H, NH); 7.61 (d, $J_{H\text{-}6/H\text{-}5}$ = 8.1Hz, 1H, H6); 5.73 (d, $J_{H5\text{-}H6}$=7.3Hz, 1H, H5); 5.68 (d, $J_{H1'\text{-}H2'}$=4.8Hz, 1H, H1´); 5.41, 5.26 (2d_{AB}, J_{AB} = 6.2Hz, 2H, OCH_2O, PivOM); 4.55 (d, J =4.9Hz, 1H, H3´) 4.39 (d, J =4.7Hz, 1H, H2´); 4.06 (m, 1H, H4´); 3.96 (dd, $^2J_{H5'/H5''}$ =12.2Hz, $^3J_{H5'/H4'}$ =2.0Hz, 1H, H5´); 3.74 (dd, $^2J_{H5'/H5''}$ =12.2Hz, $^3J_{H5'/H4'}$ =2.0Hz, 1H, H5´´); 1.17 (s, 9H, $OCOC(CH_3)_3$, PivOM); 0.91 (s, 9H, $OSiC(CH_3)_3$, TBDMS); 0.12, 0.10 (2x s,6H, $Si(CH_3)_2$, TBDMS). ^{13}C-NMR (75MHz, $CDCl_3$): δ 178.0 (OC=O); 163.3 (C=O); 150.2 (C=O); 142.3 (C6); 102.3 (C5); 91.2 (C1´); 88.1 (OCH_2O, PivOM); 85.7 (C4´); 79.6 (C2´); 69.9 (C3´); 61.1 (C5´); 38.7 ($OCOC(CH_3)_3$, Cq, PivOM); 26.9 ($OCOC(CH_3)_3$, PivOM); 25.6 ($OSiC(CH_3)_3$, TBDMS); 18.0 ($SiC(CH_3)_3$, Cq, TBDMS); -4.6, -4.9 (2x $SiC(CH_3)_2$). HRMS (ESI) Calcd for $C_{21}H_{36}N_2O_8Si$ $[M\text{-}H]^-$ 471.2163; found, 471.2160.

2´-*O*-PivOM-3´-*O*-TBDMS-5´-alkene Uridine (4)

3´-O-*tert*-butyldimethylsilyl-2´-O-Pivaloyloxymethyl Uridine (1.04g, 2.20mmol, **compound 3**) was dissolved in 195mL of acetonitrile and IBX (1.23g, 4.39mmol) was added at once as a white powder. The white suspension was heated in an oil bath to 80ºC for 1h and upon completion cooled down to r.t. The reaction mixture was filtered through a bed of celite, the celite bed was rinsed with acetonitrile (2x30mL) and the solvent removed under reduced pressure to give crude aldehyde as a white foam. After the oxidation step, the crude 5´-aldehyde-3´-O-*tert*-butyldimethylsilyl-2´-O-Pivaloyloxymethyl Uridine (1.01g, 2.13mmol) was then dissolved under Argon atmosphere in distilled THF (20mL) and cooled to 0ºC. A solution of 0.5M Tebbe reagent in toluene (8.55mL, 2eq) was added dropwise and the reaction was stirred at 0ºC for 2h. The mixture was neutralized by dropwise addition of aqueous $NaHCO_3$, filtered through a bed of celite, and the celite bed was rinsed with dichloromethane (3x15mL). The solution was washed with aqueous NaCl (45mL), dried over Na_2SO_4 and the solvent was removed under reduced pressure. Flash chromatography purification applying a stepwise gradient elution with 0-70% EtOAc in cyclohexane gave the 5´-*C*-methylene as a slightly yellowish foam in 50% overall yield (0.229g, 0.49mmol, 2-steps: oxidation + homologation) after recovery of the unreacted aldehyde (560mg, 1.18mmol). ^{1}H-NMR (300MHz, $CDCl_3$): δ 9.11 (b.s, 1H, NH); 7.32 (d, $J_{H\text{-}6/H\text{-}5}$ = 8.1Hz, 1H, H6); 5.92-5.74 (m, 3H, H1´, H5´ and H5´´); 5.47-5.30 (m, 4H, OCH_2O, H6´and H6´´); 4.40-4.32 (m, 2H, H3´ and H2´); 4.01 (m, 1H, H4´); 1.18 (s, 9H, $OCOC(CH_3)_3$, PivOM);

0.89 (s, 9H, OSiC(CH_3)$_3$, TBDMS); 0.10-0.07 (2x s,6H, Si(CH_3)$_2$, TBDMS). ^{13}C-NMR (75MHz, $CDCl_3$): δ 178.2 (OC=O); 163.3 (C=O); 149.1 (C=O); 140.4 (C6); 134.3 (C5´); 119.8 (C6´); 102.6 (C5); 90.7 (C1´); 88.4 (OCH_2O, PivOM); 84.4 (C4´); 80.8 (C2´); 74.4 (C3´); 38.9 (OCOC(CH_3)$_3$, Cq, PivOM); 27.1 (OCOC(CH_3)$_3$, PivOM); 25.7 (OSiC(CH_3)$_3$, TBDMS); 18.1 (SiC(CH_3)$_3$, Cq, TBDMS); -4.4 (SiC(CH_3)$_2$). HRMS (ESI) Calcd for $C_{22}H_{36}N_2O_7Si$ $[M-H]^-$ 467.2214; found, 467.2213.

2´-*O*-PivOM-5´-boronic acid Uridine (5)

In a 3-necked RB flask adapted with a reflux condenser, borane dimethyl sulfide complex (0.534mL, 5.6mmol) was diluted in 15mL of anhydrous ether under Argon atmosphere and the solution was heated to 34ºC. α-Pinene (1.79mL, 11.2mmol) was added dropwise and the reaction left for 4h at 34ºC. The mixture was cooled down to rt., a solution of 5´-*C*-methylene-3´-O-tert-butyldimethylsilyl uridine (0.33g, 0.70mmol) in freshly distilled THF (4mL) was added dropwise under Argon and the reaction was left at rt for overnight. An aqueous 0.1M HCl solution (0.99mL) was added dropwise, and the reaction mixture was diluted in 15mL of EA. The solution was washed with 15mL of a saturated NaCl (aq.) solution, the organic phase dried over Na_2SO_4 and the solvent removed under reduced pressure to give crude boronic 1-(2´-*O*-Pivaloyloxymethyl-3´-*O*-*tert*-butyldimethylsilyl-uridin-5´-yl)methyl acid. The crude compound was directly dissolved in MeOH (6mL) and desilylated by addition of 7.5mL of a 1M HCl (aq.) solution. Upon 1h stirring at rt, the reaction mixture was neutralized to pH 7 with a poly(4-vinylpyridine 2% cross-linked) resine. After filtration and evaporation, the residue was purified by column chromatography on silica gel using a gradient of 0-10% MeOH in DCM to give boronic 1-(uridin-2´-*O*-Pivaloyloxymethyl-5´-yl)methyl acid (183mg, 0.45mmol) (**compound 5**) in 64.9% overall yield (2 steps: borylation + desilylation). ^{1}H-NMR (300MHz, MeOD): δ 7.60 (d, $J_{H\text{-}6/H\text{-}5}$ = 8.1Hz, 1H, H6); 5.83 (d, $J_{H\text{-}1´/H\text{-}2´}$=3.4Hz, 1H, H1´); 5.74 (d, $J_{H\text{-}5/H\text{-}6}$=8.1Hz, 1H, H5); 5.46-5.34 (dd, J=6.4Hz, 2H, OCH_2O); 4.36-4.33 (m, 1H, H4´); 3.93-3.89 (m, 1H, H2´); 3.84-3.80 (m, 1H, H3´); 1.85-1.68 (m, 2H, H5´and H5´´); 1.18 (s, 9H, OCOC(CH_3)$_3$, PivOM); 0.99-0.88 (m, 2H, H6´and H6´´). ^{13}C-NMR (75MHz, MeOD): δ 179.4 (OC=O); 166.1 (C=O); 151.9 (C=O); 142.3 (C6); 102.9 (C5); 90.2 (C1´); 89.5 (OCH_2O, PivOM); 86.2 (C4´); 82.7 (C2´); 74.1 (C3´); 39.8 (OCOC(CH_3)$_3$, Cq, PivOM); 28.6 (C5´); 27.3 (OCOC(CH_3)$_3$, PivOM). ^{11}B-NMR (128MHz, MeOD): δ 31.5. HRMS (ESI) Calcd for $C_{16}H_{25}BN_2O_9Na$ $[M+Na]^+$ 423.1551; found, 423.1550.

2´-*O*-PivOM-5´-MIDA boronate Uridine (6)

Boronic 1-(uridin-2´-*O*-Pivaloyloxymethyl-5´-yl)methyl acid (69mg, 0.17mmol) was dissolved in 4mL of a (DMSO/Benzene) (1/9) (v/v) solution. The reaction was left with stirring at 110ºC for overnight on using a Dean-Stark apparatus combined with a reflux condenser. The solvent was then removed under reduced pressure on a rotary evaporator. The oily crude was subjected to purification by column chromatography using a stepwise gradient 0-10% MeOH in dichloromethane to afford **compound 6** in 74.9% yield (66mg, 0,13mmol). ^{1}H-NMR (300MHz, MeOD): δ 9.10 (bs, 1H, N-H); 7.41 (d, $J_{H\text{-}6/H\text{-}5}$ = 8.1Hz, 1H, H6); 5.81 (d, $J_{H\text{-}1'/H\text{-}2'}$=4.2Hz, 1H, H1´); 5.67 (d, $J_{H\text{-}5/H\text{-}6}$ = =8.1Hz, 1H, H5); 5.36-5.30 (dd, J=6.4Hz, 2H, OCH_2O); 4.28 (m, 1H, H4´); 3.98-3.77 (m, 6H, H2´, H3´, 2xCH_2 MIDA); 2.85 (s, CH_3, 3H, MIDA); 1.74-1.62 (m, 2H, H5´and H5´´); 1.15 (s, 9H, $OCOC(CH_3)_3$, PivOM); 0.76-0.64 (m, 2H, H6´and H6´´). ^{13}C-NMR (75MHz, MeOD): δ 178.1 (OC=O); 168.7 (C=O MIDA); 163.4 (C=O); 150.9 (C=O); 140.8 (C6); 102.6 (C5); 88.7 (C1´); 88.2 (OCH_2O, PivOM); 86.2 (C4´); 81.6 (C2´); 72.9 (C3´); 62.4 (CH_2 MIDA); 46.2 (CH_3 MIDA); 38.9 ($OCOC(CH_3)_3$, Cq, PivOM); 28.3 (C5´); 26.7 ($OCOC(CH_3)_3$, PivOM). ^{11}B-NMR (128MHz, MeOD): δ 13.1. HRMS (ESI) Calcd for $C_{21}H_{29}BN_3O_{11}$ $[M\text{-}H]^-$ 510.1895; found, 510.1904.

2´-*O*-PivOM-3´-*O*-(P-(2-cyanoethoxy-*N,N*-diisopropylaminophos-phinyl))-5´-MIDA boronate Uridine (7)

Compound 6 (50mg, 0,0978mmol) was coevaporated in anhydrous acetonitrile (3x5mL) and dissolved in 1,5mL of CH_2Cl_2 previously passed through an alumina column. To the solution was added DIEA (30µL, 0,176mmol) and *N,N*-diisopropylchlorophosphoramidite (32µL, 0,146mmol) under Argon. The mixture was stirred for 5h at rt. After reaction completion, the crude was passed directly through a silica gel column chromatography on using a gradient of 0-25% acetone in EA containing 1% of pyridine to afford the desired phosphoramidite **(7)** as a colorless oil (68mg, 0,0955mmol) in 97% yield. ^{1}H-NMR (400MHz, CD_3CN): δ 7.41 (2xd, $J_{H\text{-}6/H\text{-}5}$ = 8.1Hz, 1H, H6); 5.89 (2xd, $J_{H\text{-}1'/H\text{-}2'}$=4.5Hz, 1H, H1´); 5.66 (2xd, $J_{H\text{-}5/H\text{-}6}$ = =8.1Hz, 1H, H5); 5.39-5.20 (m, J=6.4Hz, 2H, OCH_2O); 4.41-3.61 (m, 11H, H2´, H3´, H4´, 2xCH_2 MIDA, OC*H2*CH2CN CE, OCH2C*H2*CN CE); 2.86 (2xs, CH_3, 3H, MIDA); 2.68 (m, 2H, 2xCH Pr^i); 1.84-1.63 (m, 2H, H5´and H5´´); 1.21-1.14 (m, 21H, $OCOC(CH_3)_3$ PivOM and 4xCH3 Pr^i); 0.77-0.64 (m, 2H, H6´and H6´´). ^{13}C-NMR (100MHz, CD_3CN): δ 178.1 (OC=O PivOM); 168.7 (C=O MIDA); 163.3 (C=O); 150.9 (C=O); 141.0 (C6); 119.3 (CH2CH2*CN*); 102.9 (C5); 88.7 (C1´); 87.7 (OCH_2O, PivOM); 86.1 (C4´); 80.4 (C2´); 74.5 (C3´); 62.4 (CH_2 MIDA); 59.3 (O*C*H2CH2CN CE); 46.3 (CH_3 MIDA); 43.7 (CH, NPr^i); 39.0 ($OCOC(CH_3)_3$, Cq, PivOM); 28.3 (C5´); 26.9 ($OCOC(CH_3)_3$, PivOM); 24.5 (CH3, NPr^i); 20.6 (OCH2*C*H2CN CE). ^{11}B-NMR (128MHz, CD_3CN): δ 13.0; ^{31}P-NMR (162MHz,CD_3CN): 149.6 and 149.2; HRMS (ESI) Calcd for $C_{30}H_{48}BN_5O_{12}$ $[M+H]^+$ 712.3130; found, 712.3127.

Syntheses of 5' DNA and RNA boronooligonucleotides

Syntheses were performed in 1μmol scale using an ABI 381A DNA synthesizer by phosphoramidite chemistry with conditions described in Tables S1 and S2. dT^{bn}- and U^{bn}-phosphoramidites were synthesized and incorporated at the 5'-end of an oligonucleotide sequence according to previous records.[1]

Table S1. Coupling conditions for DNA oligonucleotides syntheses.

Step	Reaction	Reagent	Time (s)
1	Deblocking	3% TCA in DCM	35
2	Coupling	0.1M amidite in CH_3CN + 0.3M BMT in CH_3CN	20
3	Capping	Ac_2O/THF/Pyridine + 10% NMI in THF	8
4	Oxidation	0.1M I_2 in THF/H_2O/Pyridine	15

Table S2. Coupling conditions for RNA oligonucleotides syntheses.

Step	Reaction	Reagent	Time (s)
1	Deblocking	3% TCA in DCM	65
2	Coupling	0.1M amidite in CH_3CN + 0.3M BMT in CH_3CN	180
3	Capping	Ac_2O/THF/Pyridine + 10% NMI in THF	160
4	Oxidation	0.1M I_2 in THF/H_2O/Pyridine	15

Analyses of 5' boronooligonucleotides

*HPLC and MALDI-TOF analysis of **ORN3** 5'-U^{bn}UUUUUU-3'*

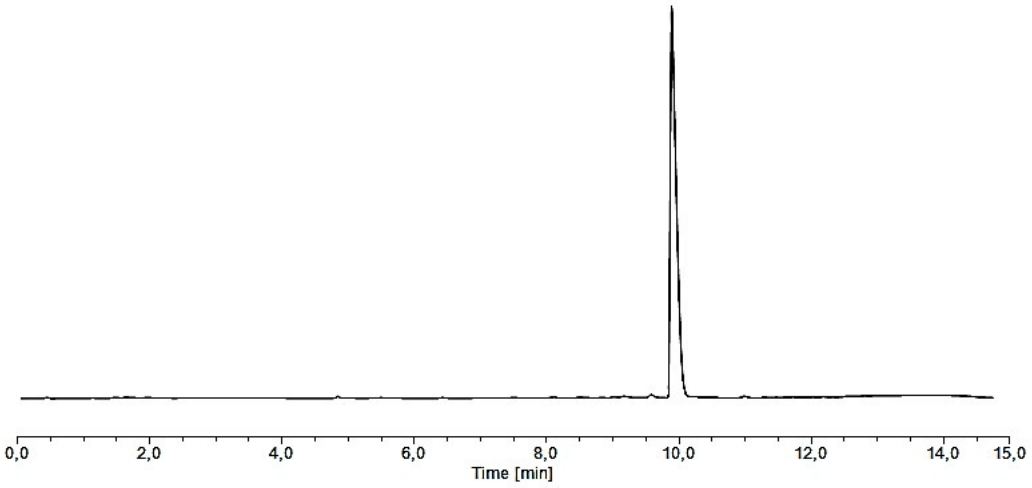

HPLC conditions analysis: Column Accucore aQ column, elution with a linear gradient of 0 to 15% CH_3CN in triethylammonium acetate buffer, pH 7, in 10,0 min, Flow rate 1.90 mL.min^{-1}, λ 260 nm.

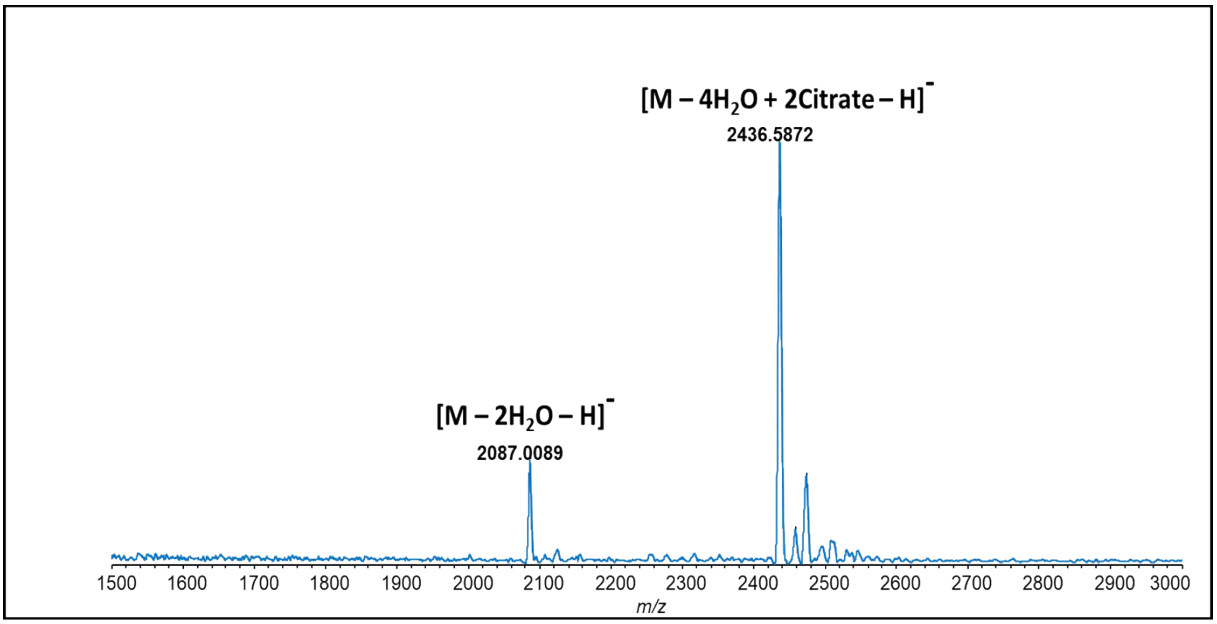

MALDI-TOF MS conditions analysis: ionization in negative mode, THAP (MW= 168.15 g.mol^{-1}) as matrix and ammonium citrate (MW= 243.2 g.mol^{-1}) as co-matrix, delay time 100 ns and an acceleration voltage of 24 kV.

*HPLC and MALDI-TOF analysis of **ORN6** 5'-U^{bn}GUGUA-3'*

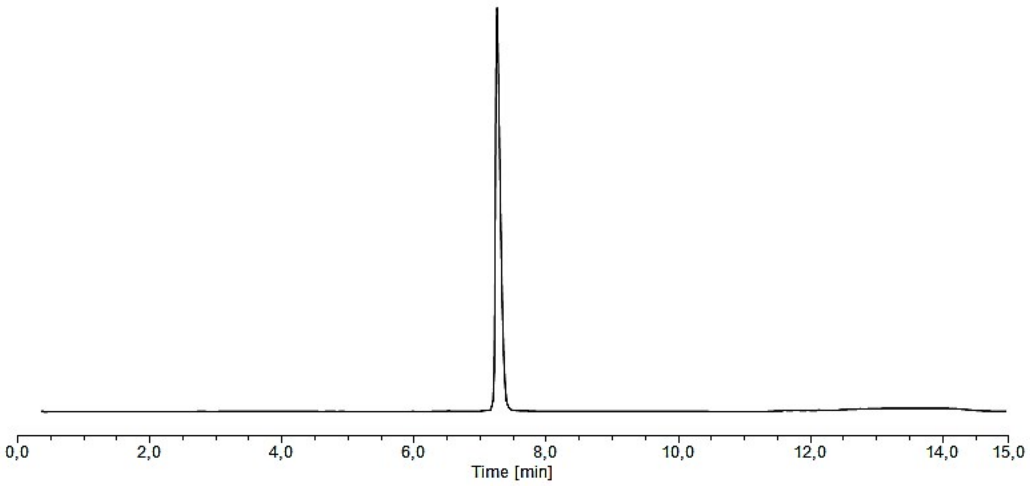

HPLC conditions analysis: Column Accucore aQ column, elution with a linear gradient of 0 to 15% CH_3CN in triethylammonium acetate buffer, pH 7, in 10,0 min, Flow rate 1.90 mL.min^{-1}, λ 260 nm.

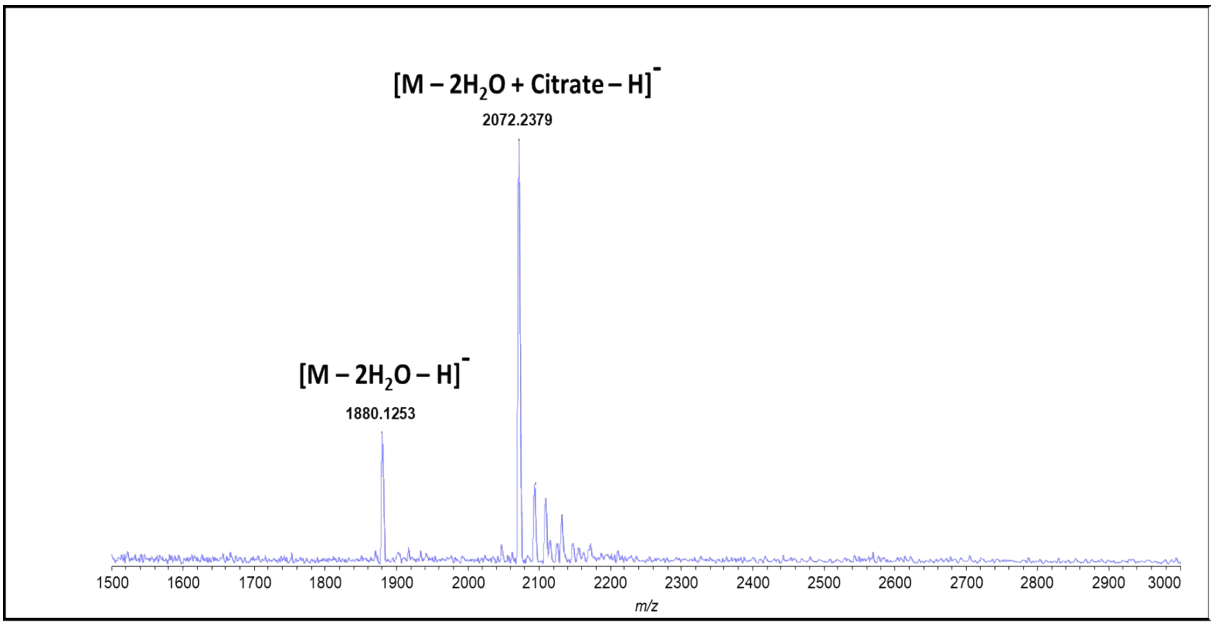

MALDI-TOF MS conditions analysis: ionization in negative mode, THAP (MW= 168.15 g.mol^{-1}) as matrix and ammonium citrate (MW= 243.2 g.mol^{-1}) as co-matrix, delay time 100 ns and an acceleration voltage of 24 kV.

Denaturation experiments

All the samples were prepared by mixing 2 μM of the template with stoichiometric amounts of their complementary strands. Denaturation experiments were performed in a 1M NaCl, 10mM sodium cacodylate buffer at pH 7.5 and 8.5. A heating-cooling-heating cycle in the 0-90°C temperature range with a gradient of 0.5°C/min was applied. Tm values were determined from the maxima of the first derivative plots of absorbance at 260 nm versus temperature.

We have previously run a few PAGE as additional experiments pertaining to DNA-templated ligation.[2] These were however done when we applied the concept to oligomerization on longer templates that led to T_m values above 20 °C. We also previously made some gels to probe the ligation between two half-strands having a T_m value of 23.8 °C whereas the control non-modified nicked duplexes had a T_m value of 12.2 °C.[1b] In contrast, when we evaluated the minimal length necessary to observe ligation, Tm values were generally below 20 °C and the resulting duplexes were not stable enough to be observed by PAGE.[3] This is the reason why we did not run any PAGE here. Indeed, in the present study we have been confronted with similar problems with either T_m values being below 20 °C or duplexes having Tm values of the same range (cf Table 2, entries 7 and 8 with a T_m value of 30.9 for the 5'-boronic modified duplex and T_m = 25.6 °C for the unmodified nicked duplex), both preventing the observation of retarded bands.

Similarly, considering the size of the different reversible loops, we cannot expect the loop structures to survive native gels. MALDI-TOF experiments do not represent, a reliable method to probe the templated ligation, as the ligation might well take place within the source as evidenced by THAP-adducts observed with 5'-boronic acid sequences.

Finally, under standard HPLC conditions, the duplex won't be stable and this will lead to denaturation with concomitant switch of the equilibrium towards the boronic acid.

Table S3. UV Thermal denaturation data.

Entry	Duplex	Template/ Complementary Sequences[a]	T_m [°C][b] pH 7.5	pH 8.5
1	ORN**1**/ORN**2**	5′-AAAAAAAGCGACGG CGCUGCC-5′	48.8	49.7
2	ODN**1**/ORN**2**	5′-**AAAAAAAGCGACGG** CGCUGCC-5′	31.7	31.7
3[c]	ODN**1**/ORN**3**/ORN**2**	5′-**AAAAAAAGCGACGG** 3′-UUUUUUU^{bn}/CGCUGCC-5′	<5	<5
4[c]	ODN**1**/ORN**4**/ORN**2**	5′-**AAAAAAAGCGACGG** 3′-UUUUUUU/CGCUGCC-5′	<5	<5
5	ORN**11**/ORN**3**	5′-AAAAAAAGCGACGG 3′-UUUUUUU^{bn}	14.7	13.7
6	ORN**12**/ORN**3**	5′-AAAAAAAGCGACGG 3′-UUUUUUU^{bn}	<5	<5
7	ORN**13**/ORN**3**	5′-AAAAAAAGCGACGG 3′-UUUUUUU^{bn}	<5	<5
8	ORN**14**/ORN**3**	5′-AAAAAAAGCGACGG 3′-UUUUUUU^{bn}	<5	<5
9	ORN**15**/ORN**3**	5′-AAAAAAAGCGACG 3′-UUUUUUU^{bn}	<5	<5
10	ORN**16**/ORN**6**	5′-CCUACACAACACAUC 3′-AUGUGU^{bn}	28.0	27.9
11	ORN**17**/ORN**6**	5′-CCUACACAACACAU 3′-AUGUGU^{bn}	27.8	26.7
12	ORN**18**/ORN**6**	5′-CCUACACAACACAUCCC 3′-AUGUGU^{bn}	29.9	28.8

[a] U^{bn} refers to boronouridine **7** and T^{bn} to boronothymidine.[1a] Bold letters represent 2′-deoxynucleotides residues. 2′-OMe residues are underlined. [b] Melting temperatures are obtained from the maxima of the first derivatives of the melting curve (ΔA_{260} *vs*. temperature) recorded in a buffer containing 1M NaCl and 10 mM of sodium cacodylate, 3 µM of each strand. Curve fits data were averaged from fits of three denaturation curves. [c] T_m values indicated refer only to the lowest temperature-dependant transition. [d] Data extracted from reference [1b].

Melting curves and their derivatives from Table S3.

Table S3, entry 1 : ORN1/ORN2

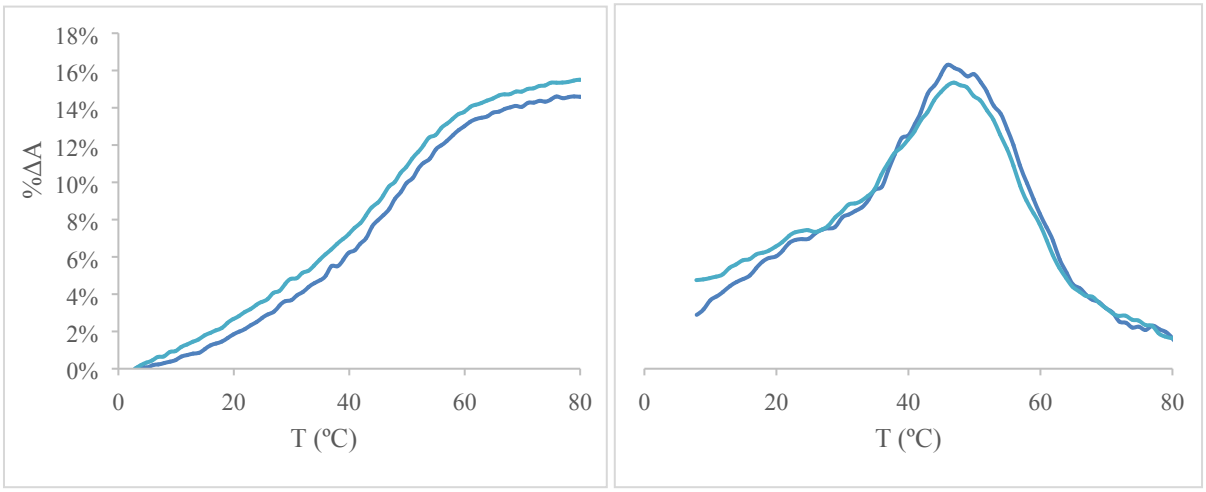

Melting curves and their derivatives at pH 7.5 (blue) and 8.5 (cyan) of the complex 5′-AAAAAAAGCGACGG-3′ with 3'- CGCUGCC-5′.

Table S3, entry 2 : ODN1/ORN2

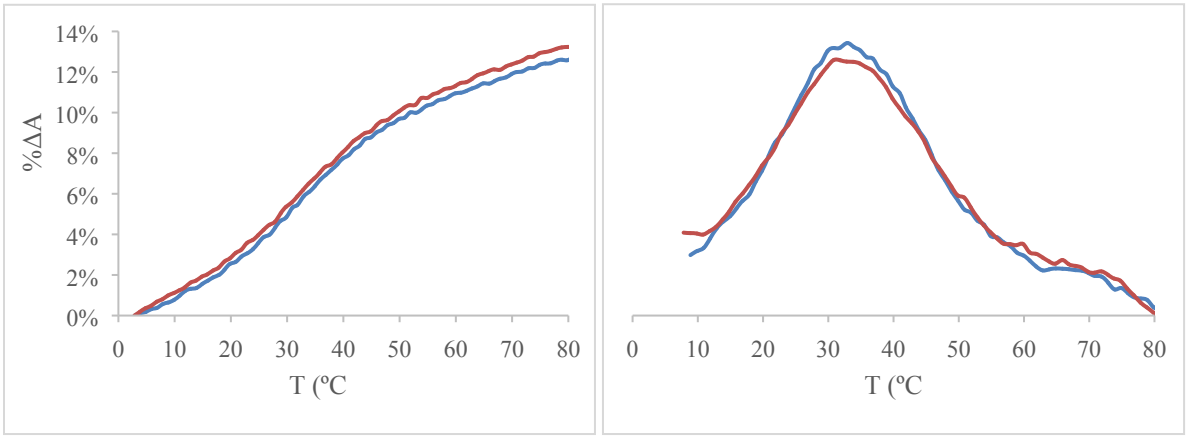

Melting curves and their derivatives at pH 7.5 (blue) and 8.5 (red) of the complex 5′-**AAAAAAAGCGACGG**-3′ with 3'- CGCUGCC-5′.

Table S3, entry 3 : ODN1/ORN3/ORN2

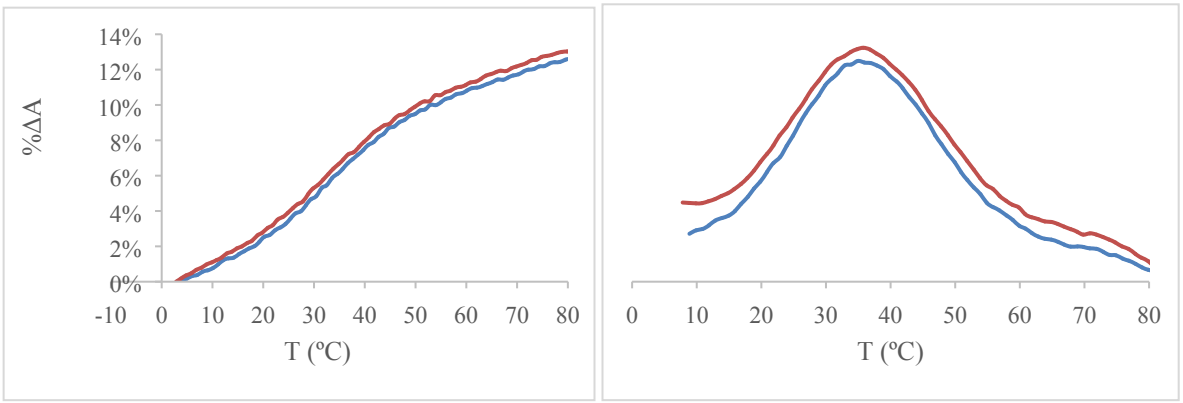

Melting curves and their derivatives at pH 7.5 (blue) and 8.5 (red) of the complex 5′-**AAAAAAAGCGACGG**-3′ with 3'-UUUUUUU^{bn}-5′ and 3′-CGCUGCC-5′.

Table S3, entry 4 : ODN1/ORN4/ORN2

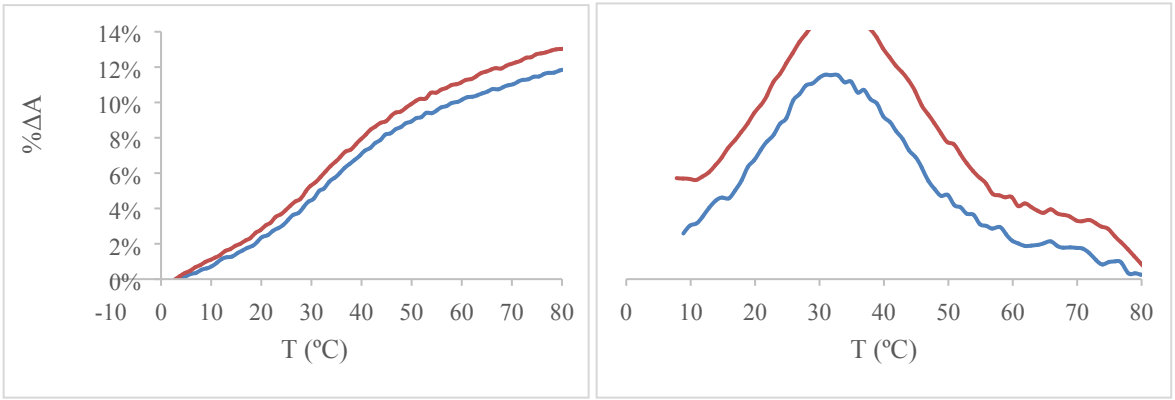

Melting curves and their derivatives at pH 7.5 (blue) and 8.5 (red) of the complex 5′-**AAAAAAAGCGACGG**-3′ with 3'-UUUUUUU-5′ and 3′-CGCUGCC-5′.

Table S3, entry 5 : ORN11/ORN3

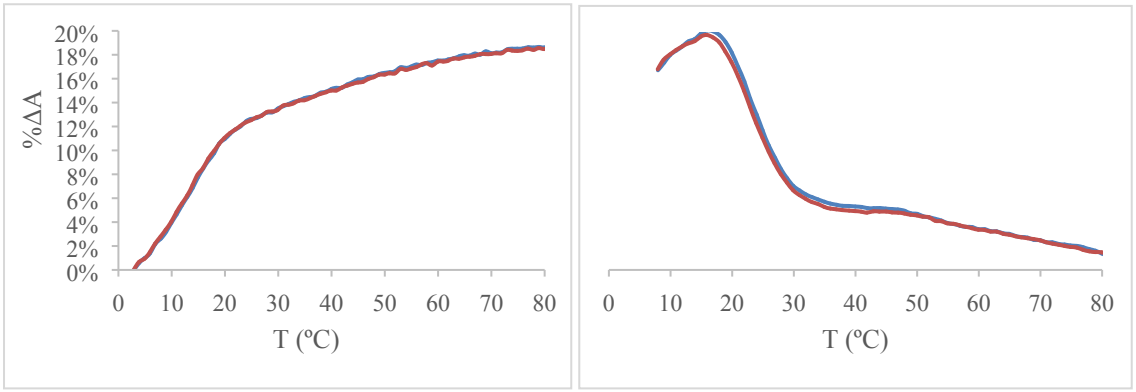

Melting curves and their derivatives at pH 7.5 (blue) and 8.5 (red) of the complex 5′-AAAAAAAGCGACGG-3′ with 3'-UUUUUUU^{bn}-5′

Table S3, entry 6 : ORN12/ORN3

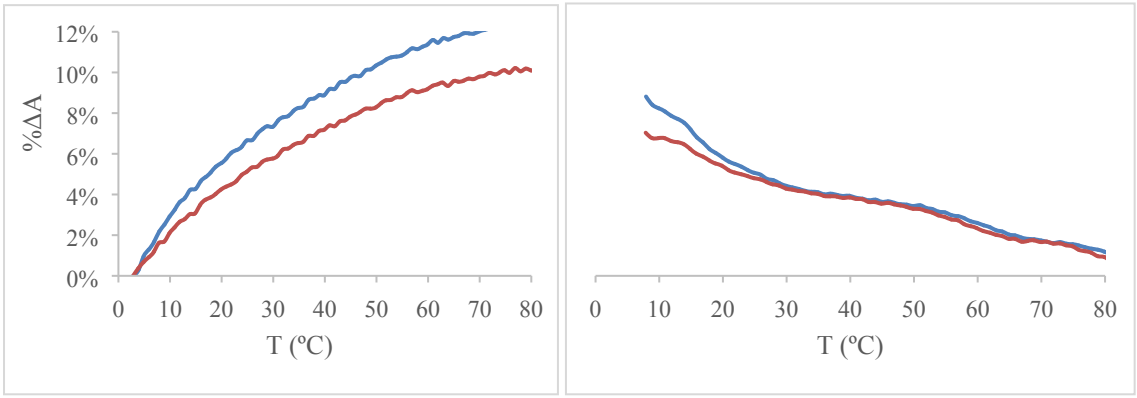

Melting curves and their derivatives at pH 7.5 (blue) and 8.5 (red) of the complex 5′-AAAAAAAGCGACGG-3′ with 3'-UUUUUUU^{bn}-5′

Table S3, entry 7 : ORN13/ORN3

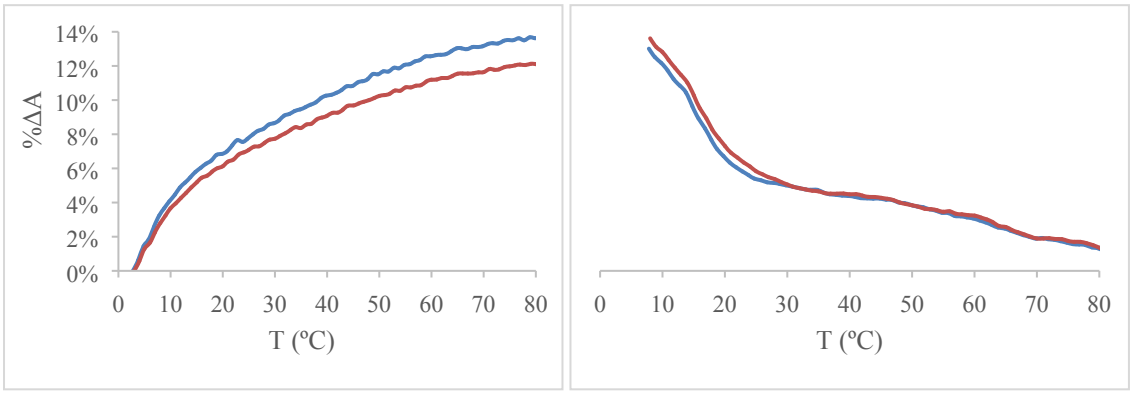

Melting curves and their derivatives at pH 7.5 (blue) and 8.5 (red) of the complex 5´-AAAAAAAGCGACGG-3´ with 3'-UUUUUUU^{bn}-5´

Table S3, entry 8 : ORN14/ORN3

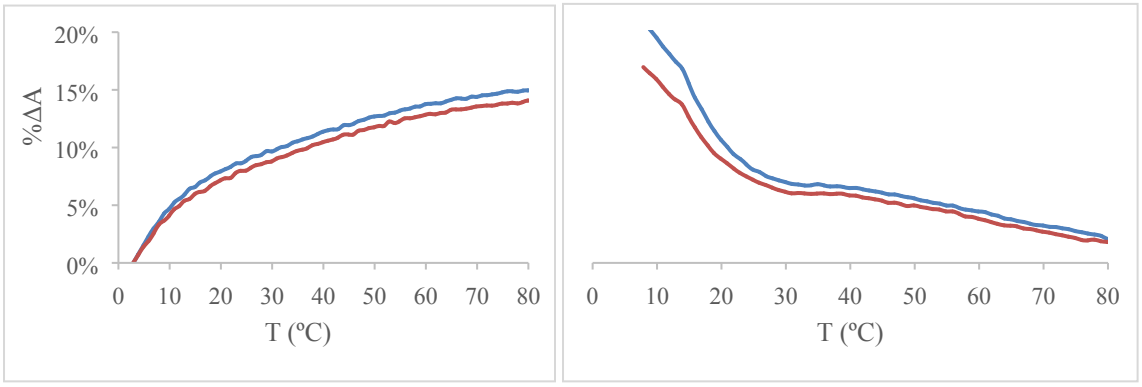

Melting curves and their derivatives at pH 7.5 (blue) and 8.5 (red) of the complex 5´-AAAAAAAGCGACGG-3´ with 3'-UUUUUUU^{bn}-5´

Table S3, entry 9 : ORN15/ORN3

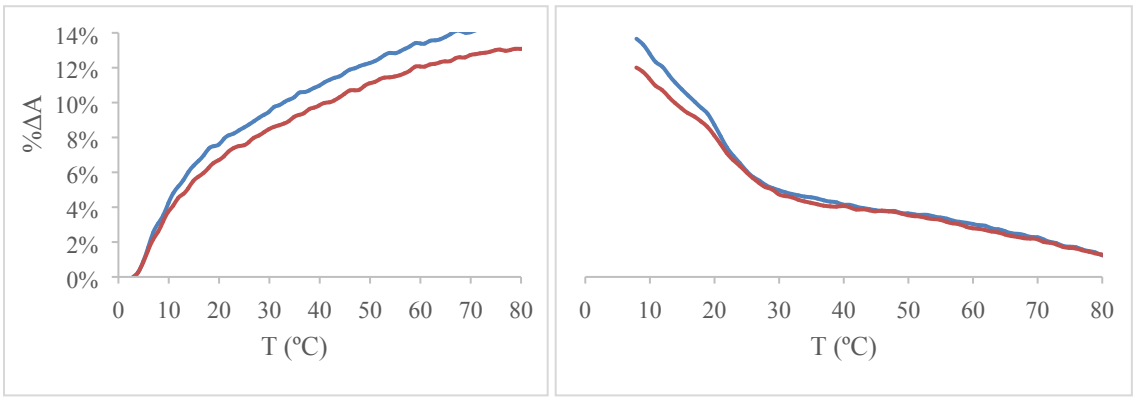

Melting curves and their derivatives at pH 7.5 (blue) and 8.5 (red) of the complex 5´-AAAAAAAGCGACG-3´ with 3'-UUUUUUU^{bn}-5´

Table S3, entry 10 : ORN16/ORN6

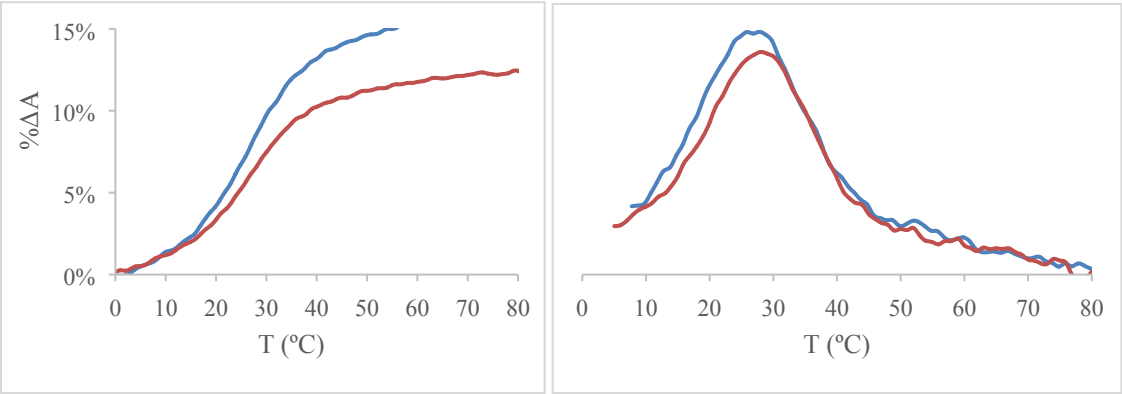

Melting curves and their derivatives at pH 7.5 (blue) and 8.5 (red) of the complex 5′-CCUACACAACACAUC-3′ with 3'-AUGUGU^{bn}-5′.

Table S3, entry 11 : ORN17/ORN6

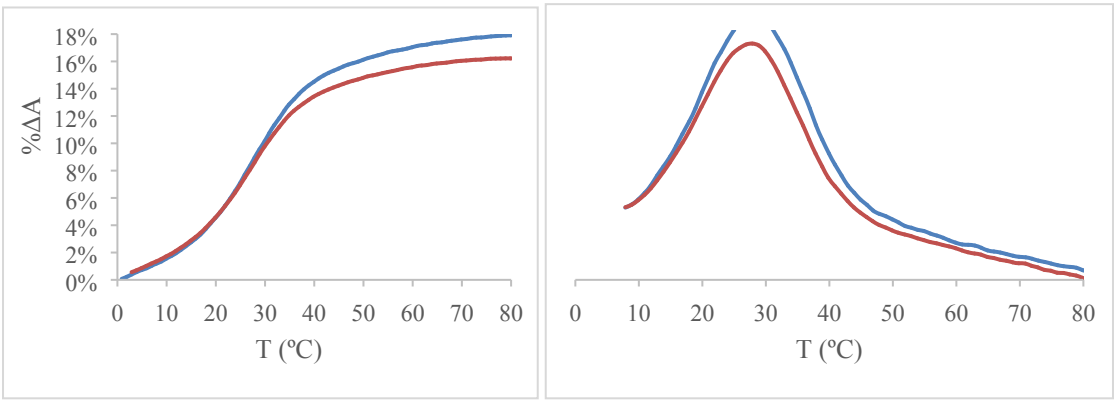

Melting curves and their derivatives at pH 7.5 (blue) and 8.5 (red) of the complex 5′-CCUACACAACACAU-3′ with 3'-AUGUGU^{bn}-5′.

Table S3, entry 12 : ORN18/ORN6

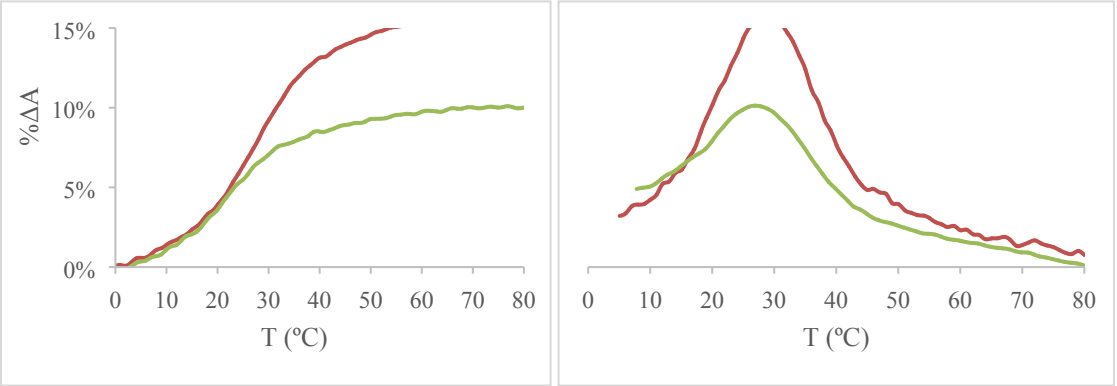

Melting curves and their derivatives at pH 7.5 (red) and 8.5 (green) of the complex 5′-CCUACACAACACAUCCC-3′ with 3'-AUGUGU^{bn}-5′.

Melting curves and their derivatives from Table 2 (Main text).

Table 2, entry 1 : ORN1/ORN3/ORN2

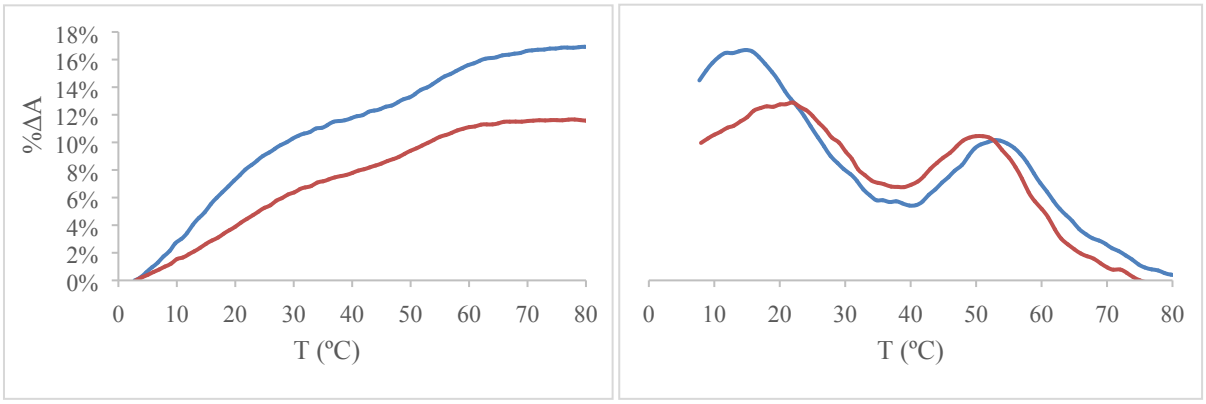

Melting curves and their derivatives at pH 7.5 (blue) and 8.5 (red) of the complex 5′-AAAAAAAGCGACGG-3′ with 3'-UUUUUUU^{bn}-5′ and 3′-CGCUGCC-5′.

Table 2, entry 2 : ORN1/ORN4/ORN2

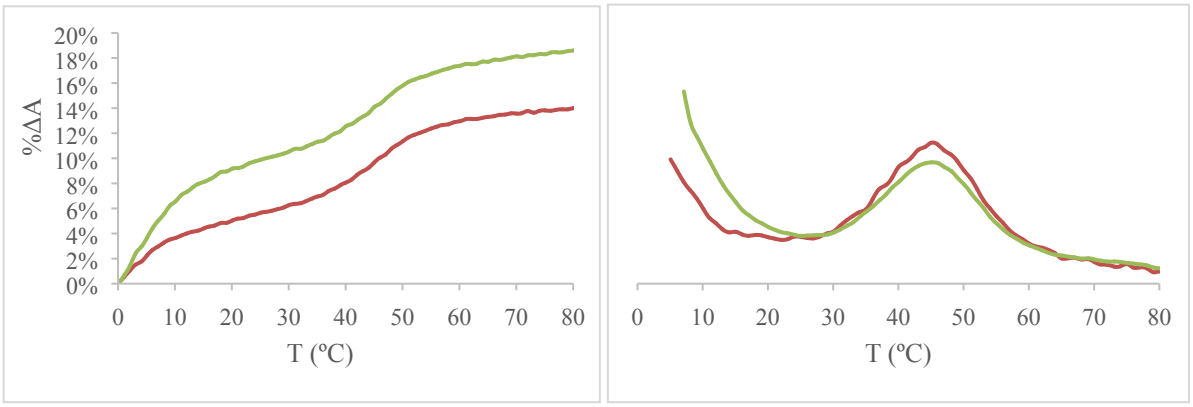

Melting curves and their derivatives at pH 7.5 (green) and 8.5 (red) of the complex 5′-AAAAAAAGCGACGG-3′ with 3'-UUUUUUU-5′ and 3′-CGCUGCC-5′.

Table 2, entry 3 : ORN5/ORN6

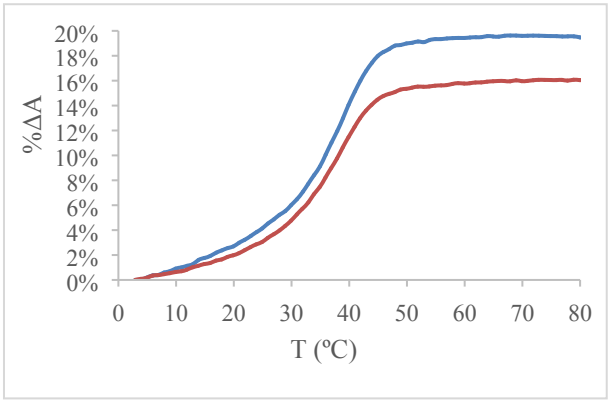

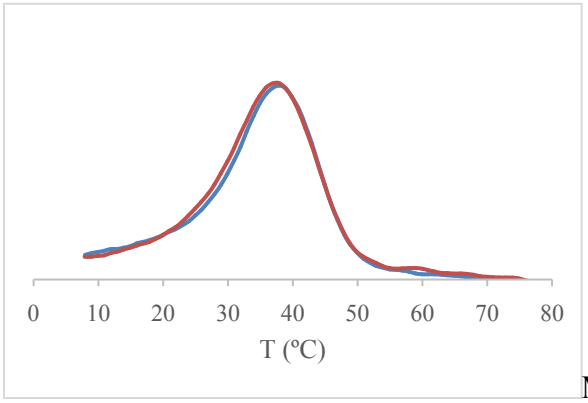

Melting curves and their derivatives at pH 7.5 (blue) and 8.5 (red) of the complex 5′-CCUACACAUACACACC-3′ with 3'-AUGUGU^{bn}-5′.

Table 2, entry 4 : ORN5/ORN7

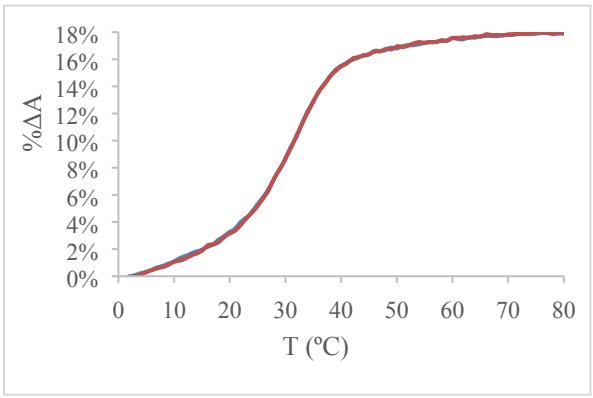

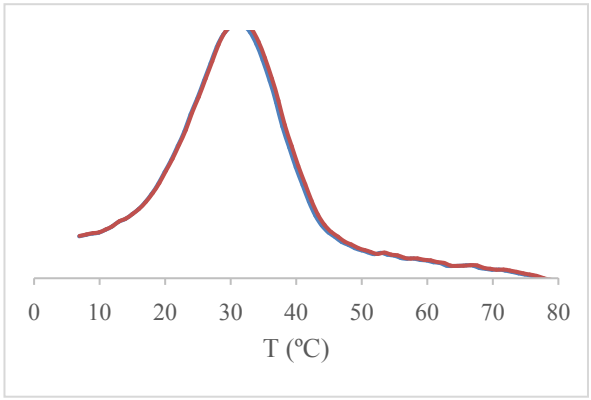

Melting curves and their derivatives at pH 7.5 (blue) and 8.5 (red) of the complex 5′-CCUACACAUACACACC-3′ with 3'-AUGUGU-5′.

Table 2, entry 5: ODN2/ORN6

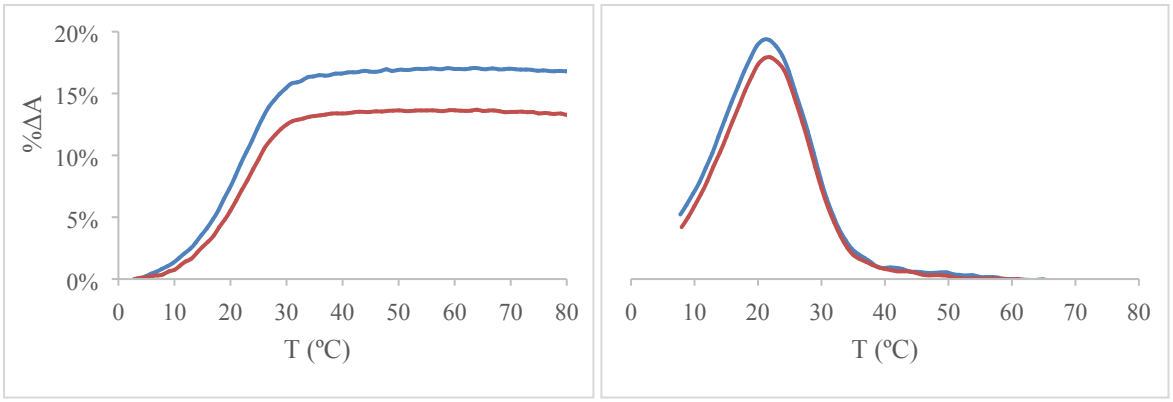

Melting curves and their derivatives at pH 7.5 (blue) and 8.5 (red) of the complex 5′-**CCTACACATACACACC**-3′ with 3'-AUGUGU^{bn}-5′.

Table 2, entry 6: ODN2/ORN7

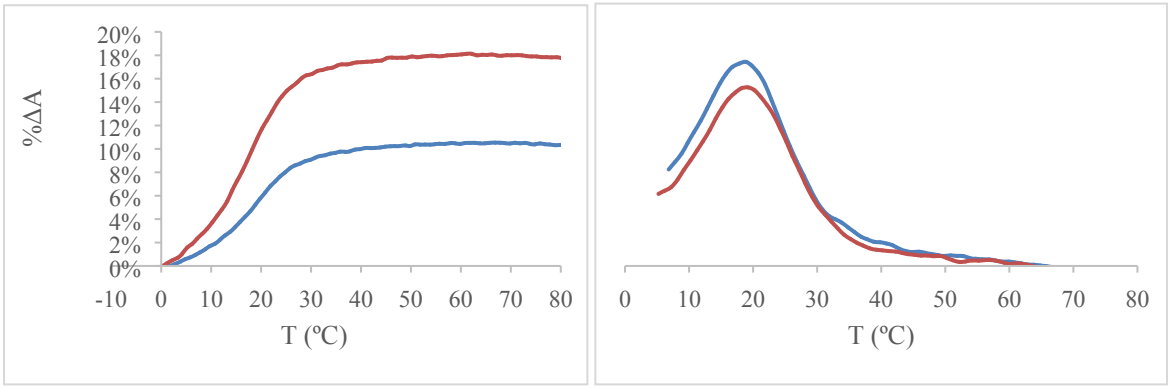

Melting curves and their derivatives at pH 7.5 (blue) and 8.5 (red) of the complex 5′- **CCTACACATACACACC** -3′ with 3'-AUGUGU-5′.

Table 2, entry 7: ORN8/ORN6

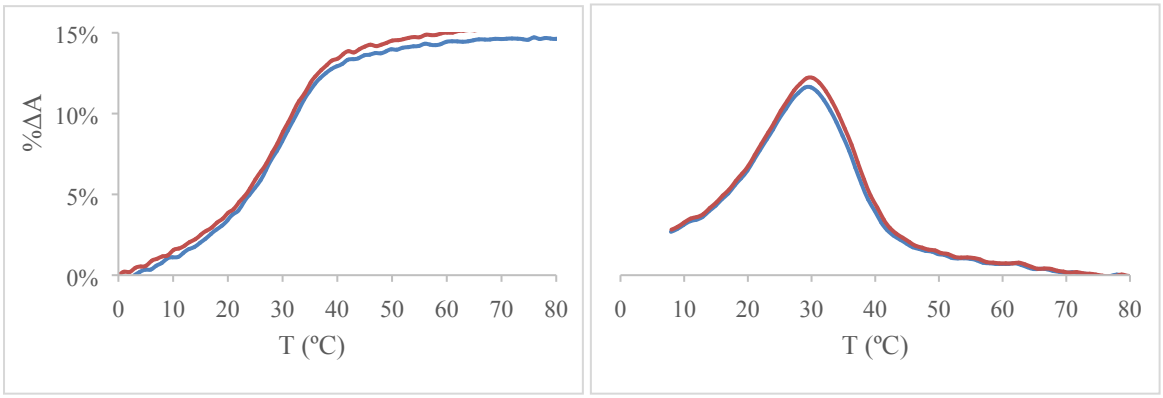

Melting curves and their derivatives at pH 7.5 (blue) and 8.5 (red) of the complex 5′-CCUACACAACACAUCC-3′ with 3'-AUGUGU^{bn}-5′.

Table 2, entry 8: ORN8/ORN7

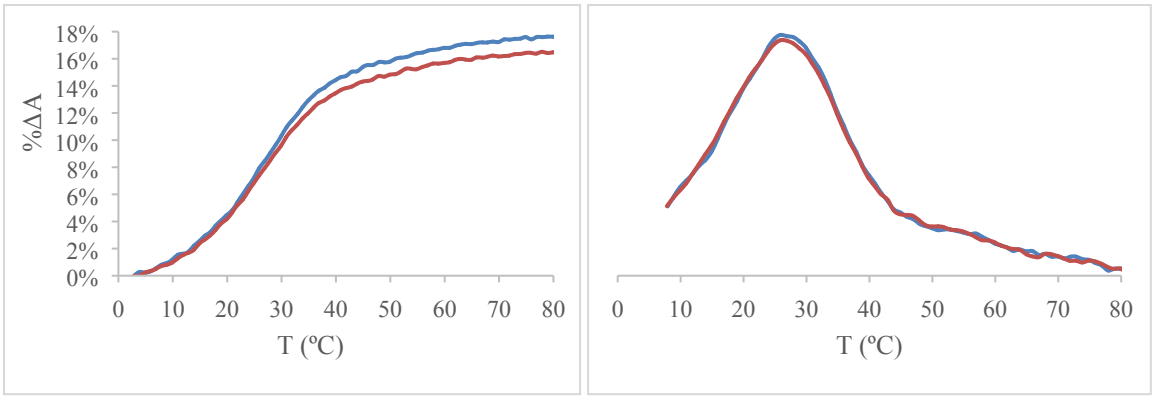

Melting curves and their derivatives at pH 7.5 (blue) and 8.5 (red) of the complex 5′-CCUACACAACACAUCC-3′ with 3'-AUGUGU-5′.

Table 2, entry 9: ORN9/ORN6

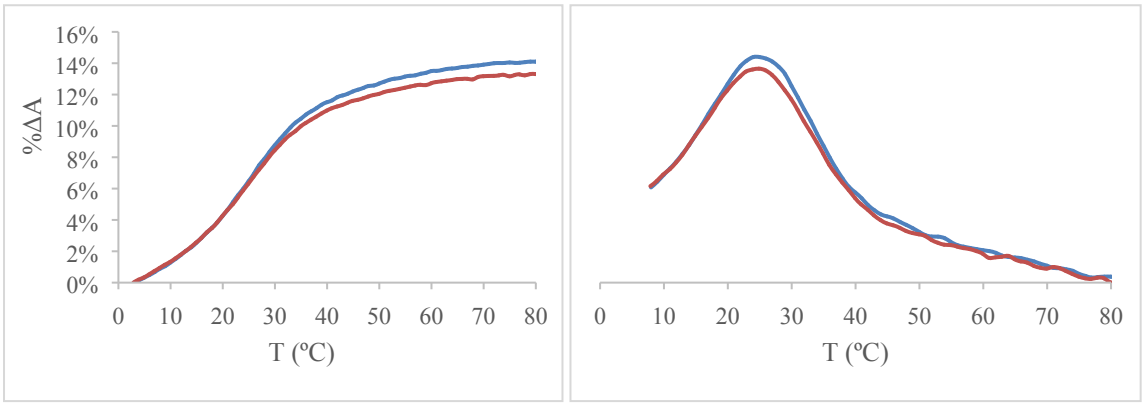

Melting curves and their derivatives at pH 7.5 (blue) and 8.5 (red) of the complex 5′-CCUACACAACACAUCC-3′ with 3'-AUGUGU^{bn}-5′.

Table 2, entry 10: ORN9/ORN7

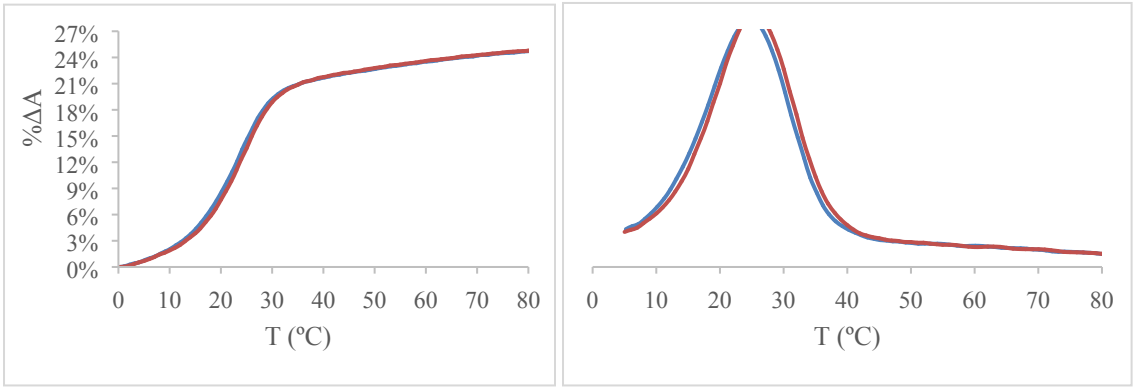

Melting curves and their derivatives at pH 7.5 (blue) and 8.5 (red) of the complex 5′-CCUACACAACACAUCC-3′ with 3'-AUGUGU-5′.

Table 2, entry 11: ORN1/ORN3

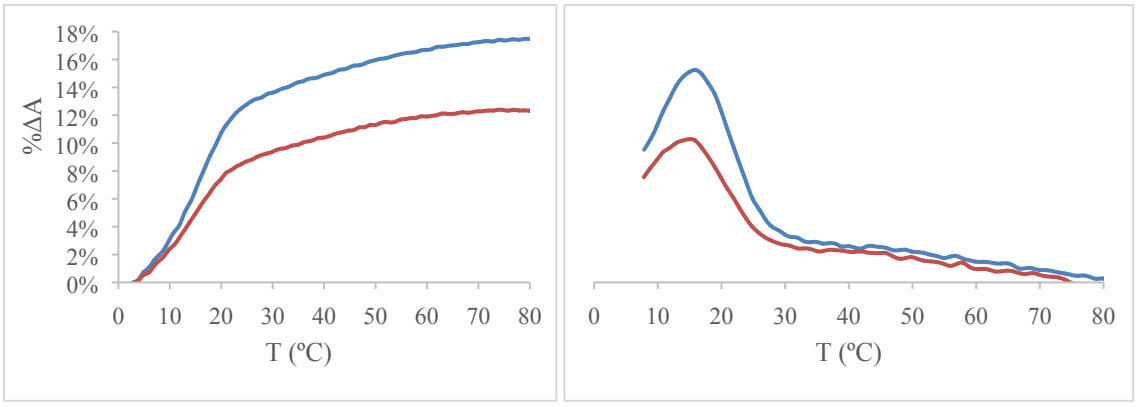

Melting curves and their derivatives at pH 7.5 (blue) and 8.5 (red) of the complex 5′-AAAAAAAGCGACGG-3′ with 3'-UUUUUUU^{bn}-5′

Table 2, entry 12: ORN1/ORN4

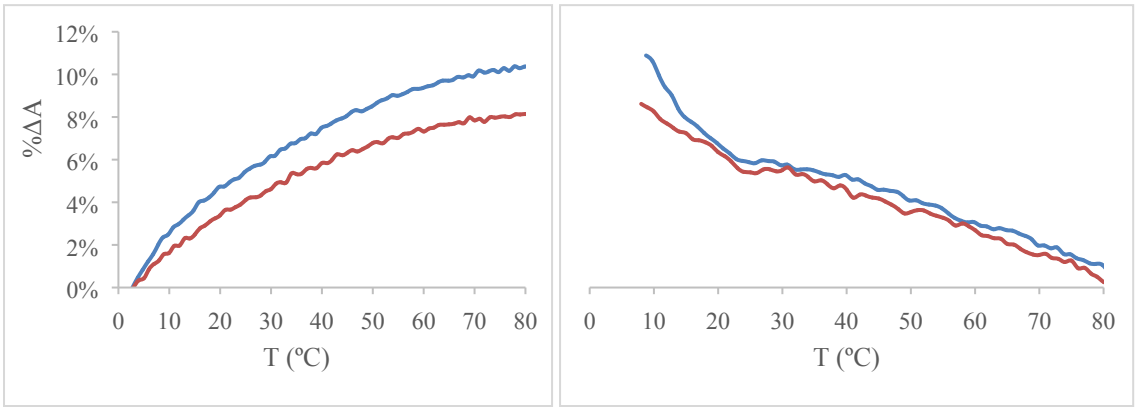

Melting curves and their derivatives at pH 7.5 (blue) and 8.5 (red) of the complex 5′-AAAAAAAGCGACGG-3′ with 3'-UUUUUUU-5′

Table 2, entry 13: ORN10/ORN3

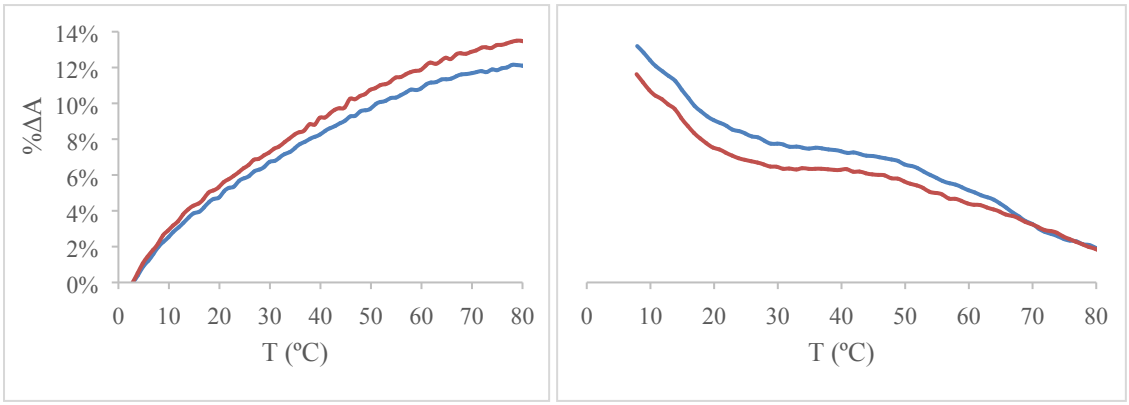

Melting curves and their derivatives at pH 7.5 (blue) and 8.5 (red) of the complex 5′-AAAAAAAGCGACGG-3′ with 3'-UUUUUUU^{bn}-5′

Table 2, entry 14: ORN10/ORN4

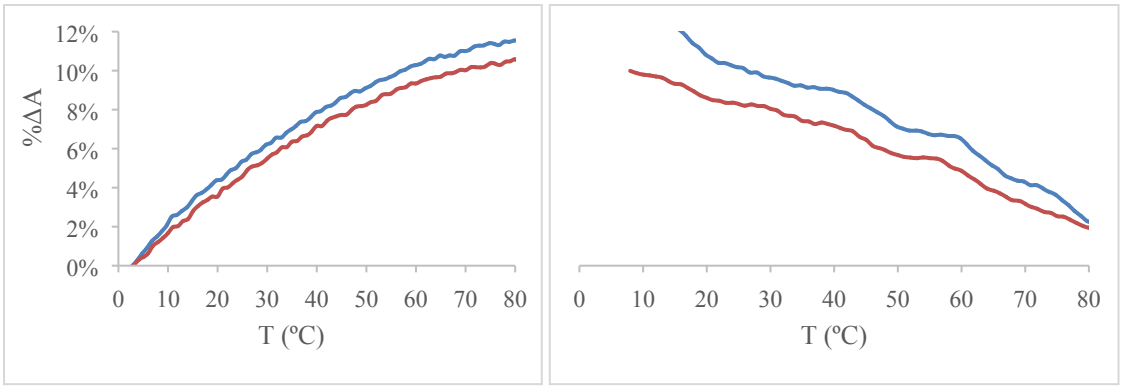

Melting curves and their derivatives at pH 7.5 (blue) and 8.5 (red) of the complex 5′-AAAAAAAGCGACGG-3′ with 3'-UUUUUUU-5′

Table 2, entry 15: ODN1/ODN3

Data extracted from previous published studies.[1b]

Table 2, entry 16: ODN1/ODN4

Data extracted from previously published studies.[1b]

Table 2, entry 17: ODN5/ODN3

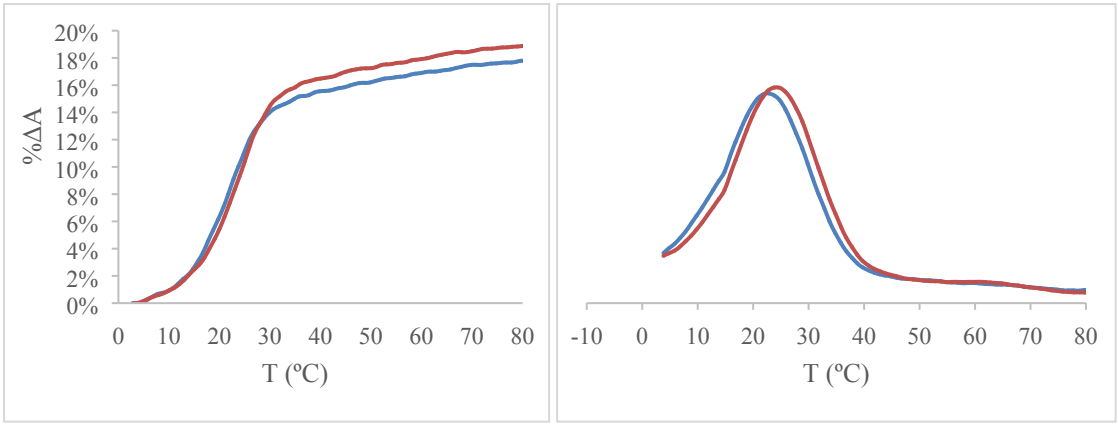

Melting curves and their derivatives at pH 7.5 (blue) and 8.5 (red) of the complex 5′-**AAAAAAAGCGACG**G-3′ with 3'-**TTTTTTT**$^{\mathbf{bn}}$-5′

MD Simulations

3D structures of nucleic acids were built using a DNA structure modelling server 3D-DART[4] that enables to create both B- as well as A- form duplexes (i.e. with either 2'-endo or 3'-endo conformers of deoxyriboses). When needed, duplex structures were edited by means of the Molefacture plugin from the VMD 1.9.3 software package (among other things, the 2'-hydroxyl groups were added to all RNA strands).[5] Nucleic acids parametrized using the CHARMM force field[6] were surrounded by TIP3P water molecules.[7] MD trajectories were produced using the NAMD 2.12 software package[8] by means of the NVIDIA graphical processing units. The smooth Particle-mesh Ewald (PME) method was employed for long-range electrostatic forces.[9] The non-bonded cutoff was set to 12 Å. The SHAKE algorithm was applied to constrain bonds where the hydrogen atoms were involved.[10] After reaching the energy minimum of simulated systems, the Langevin dynamics was used for a temperature control with target temperature set to 310 K. The Langevin piston method was applied to reach an efficient pressure control with target pressure set to 1 atm. The integration time step was set to 2 fs. MD simulations lasted for 5 ns. MD trajectories were analyzed with the aid of the VMD software package (2). Figures were produced by means of the UCSF Chimera software package (https://www.cgl.ucsf.edu/chimera/).

Figure S1. Root Mean Square Deviation

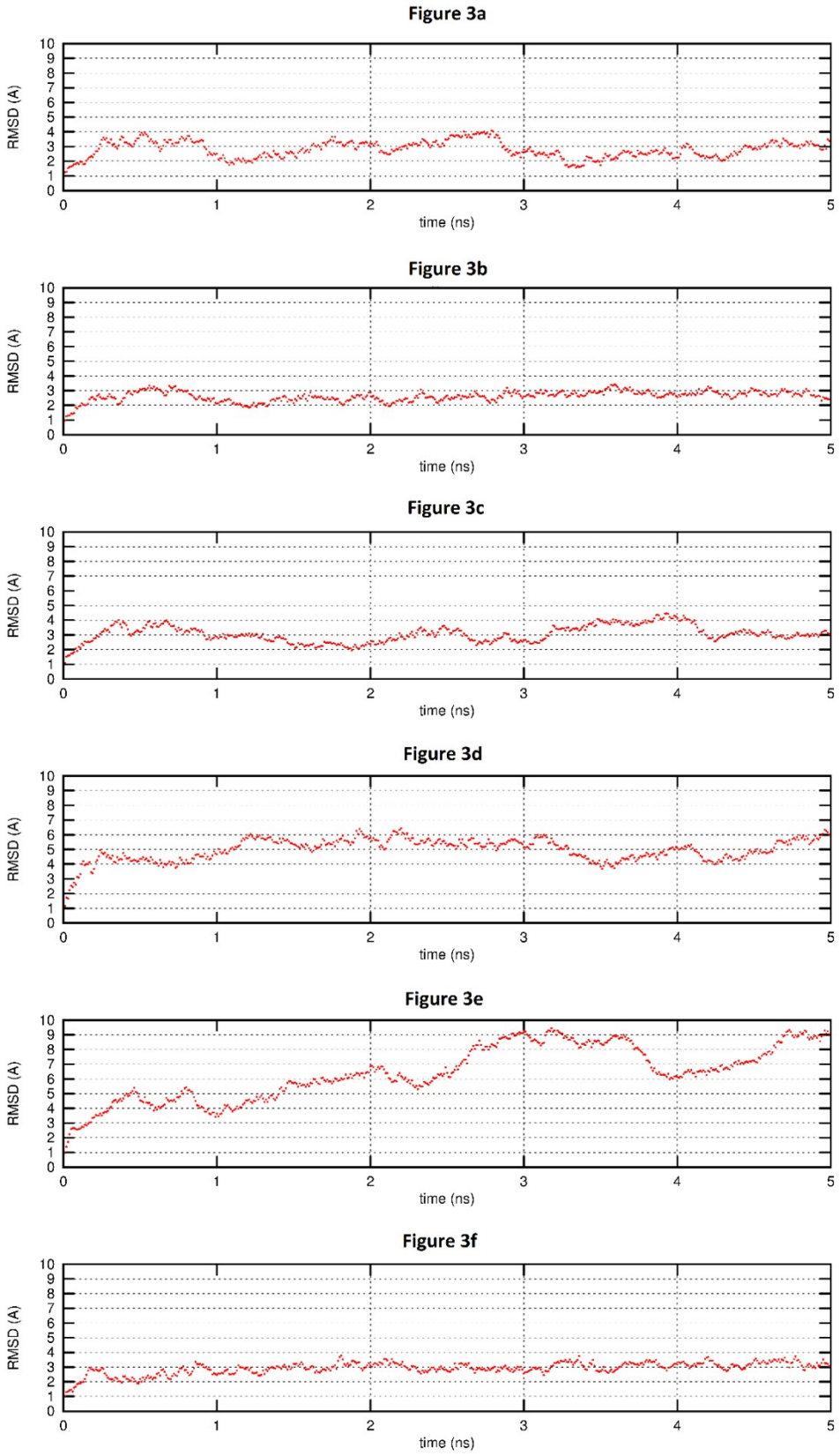

^{1}H NMR spectrum of **compound 2**

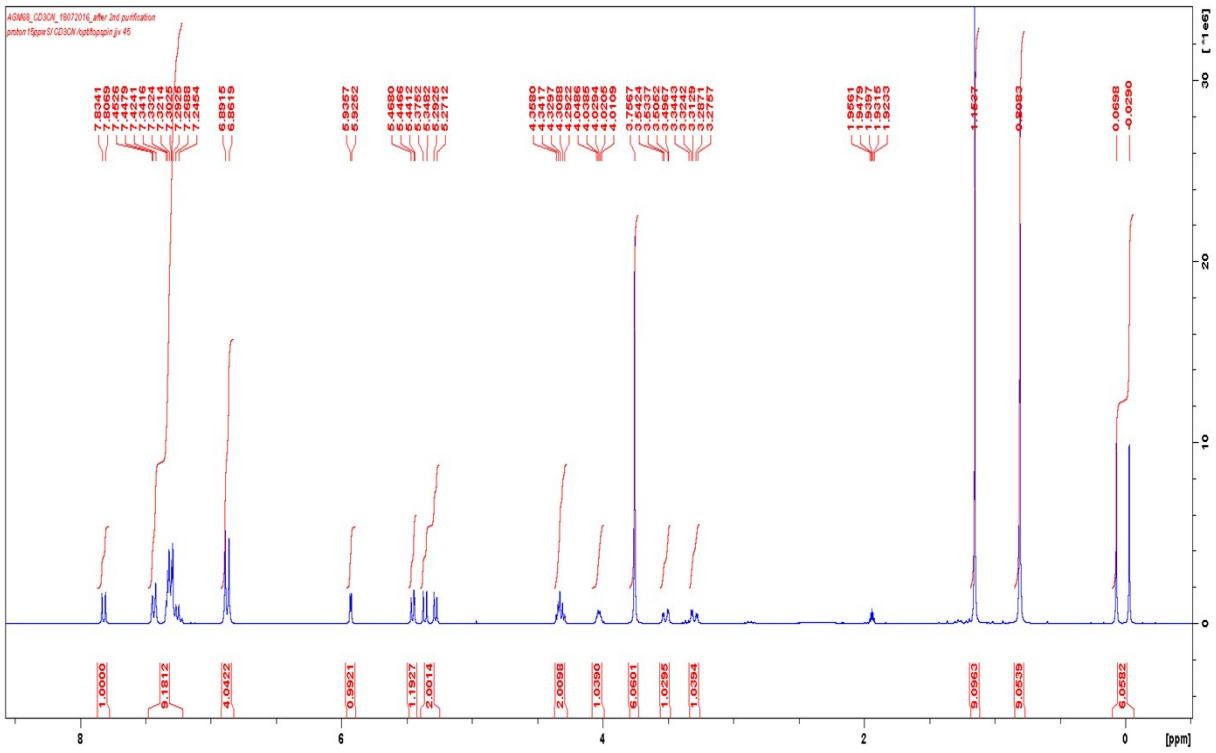

^{13}C NMR spectrum of **compound 2**

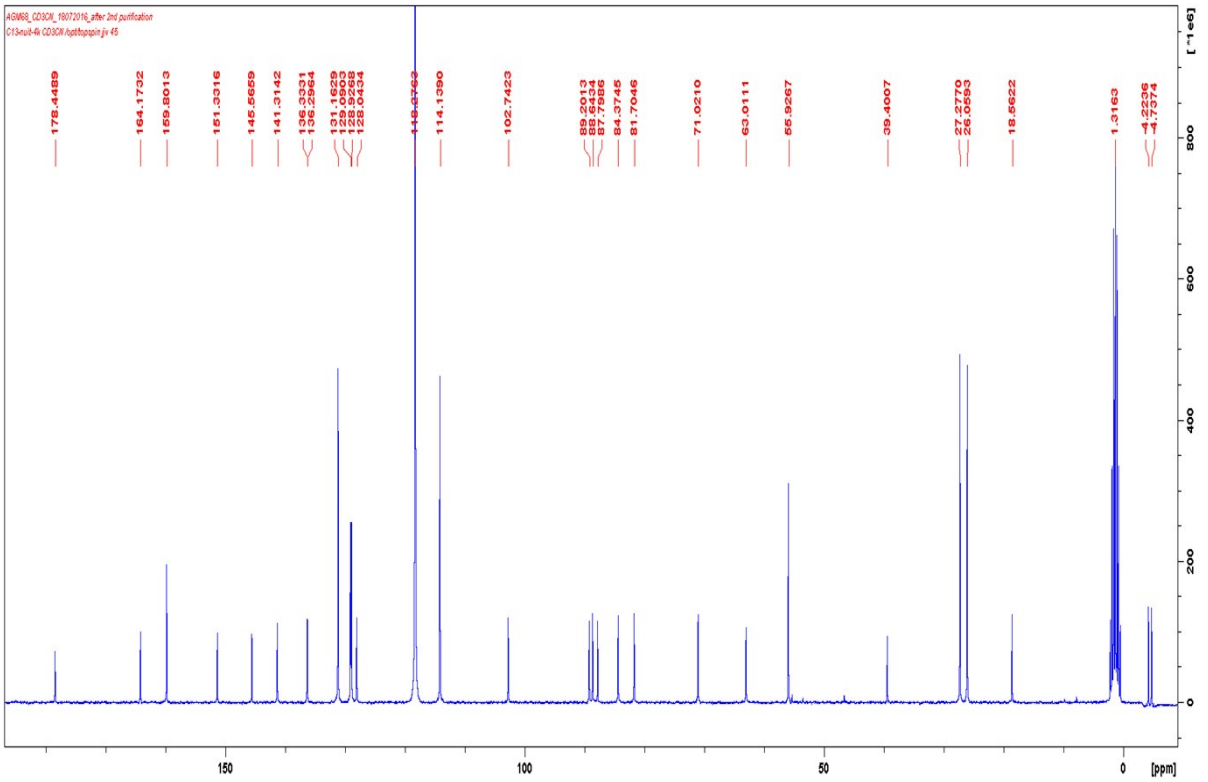

^{1}H NMR spectrum of **compound 3**

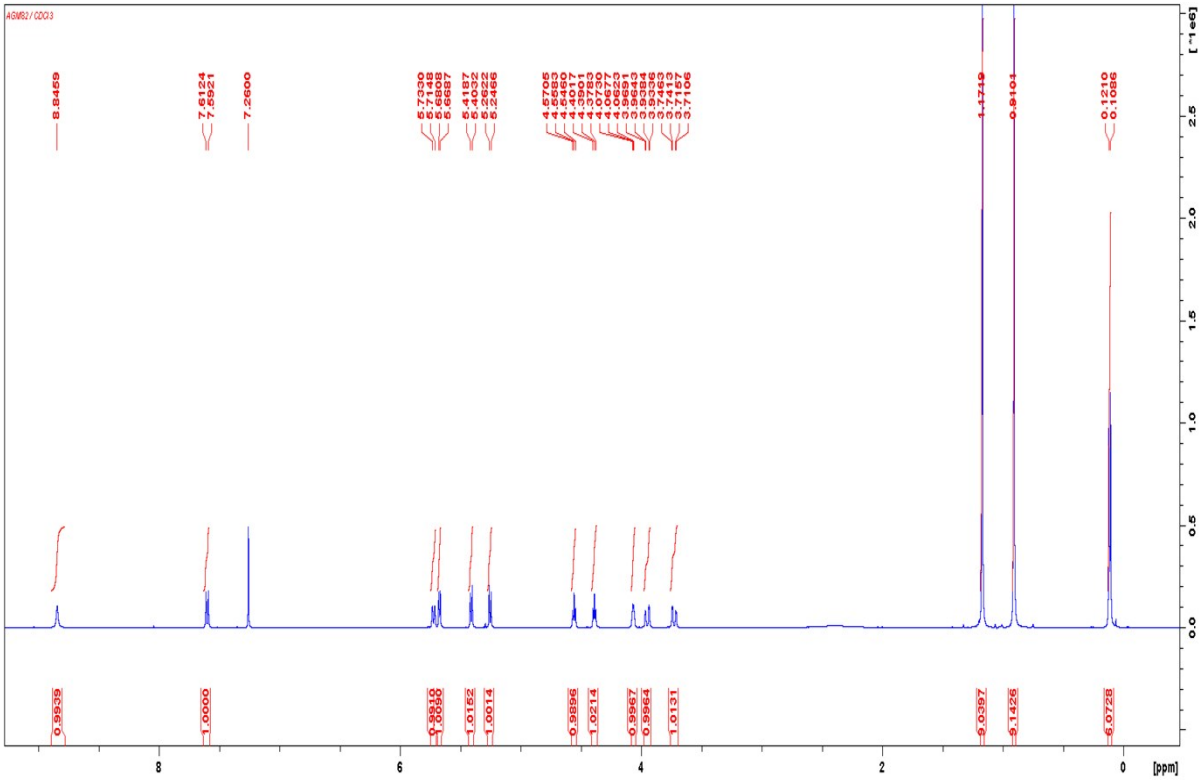

^{13}C NMR spectrum of **compound 3**

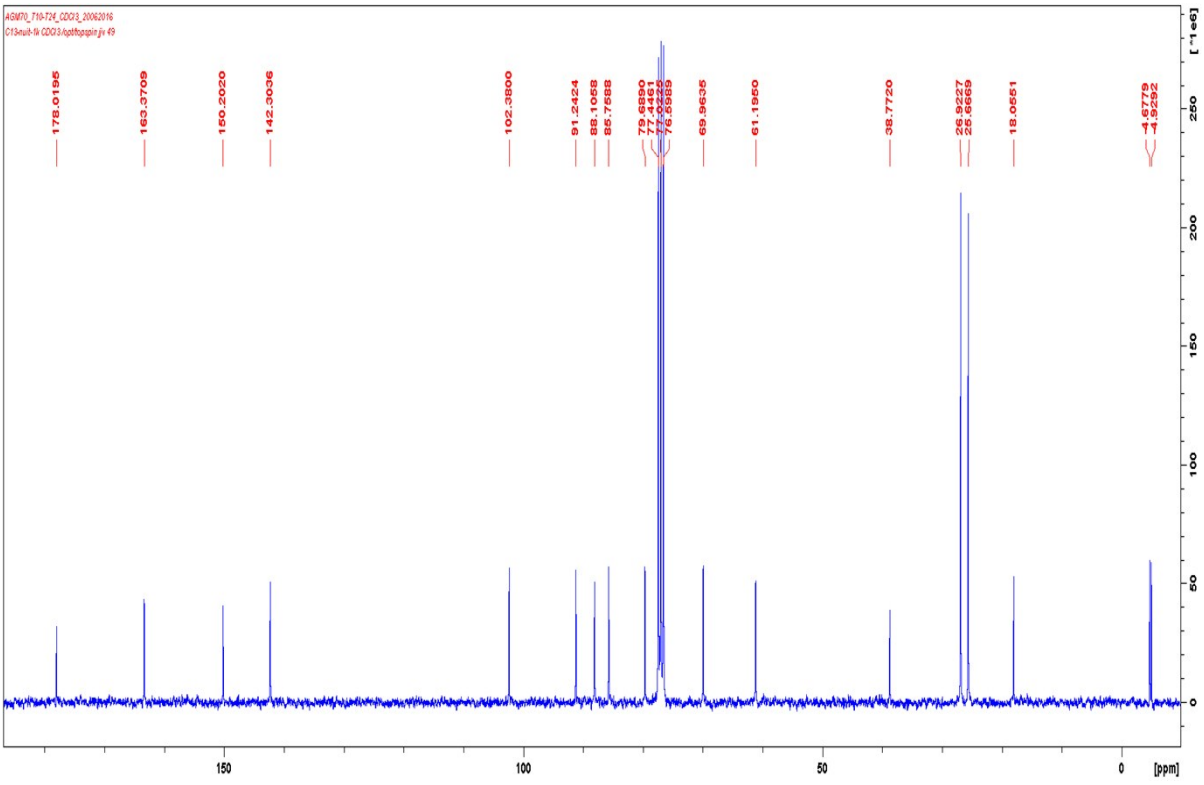

^{1}H NMR spectrum of **compound 4**

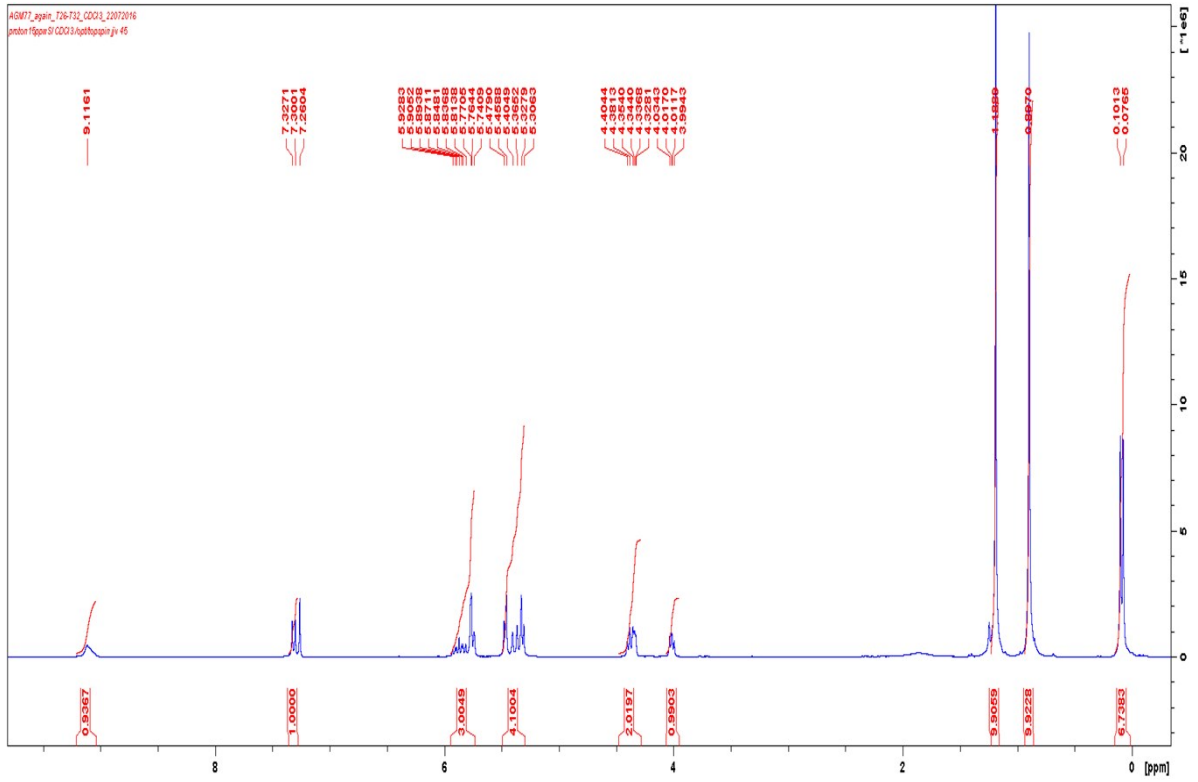

^{13}C NMR spectrum of **compound 4**

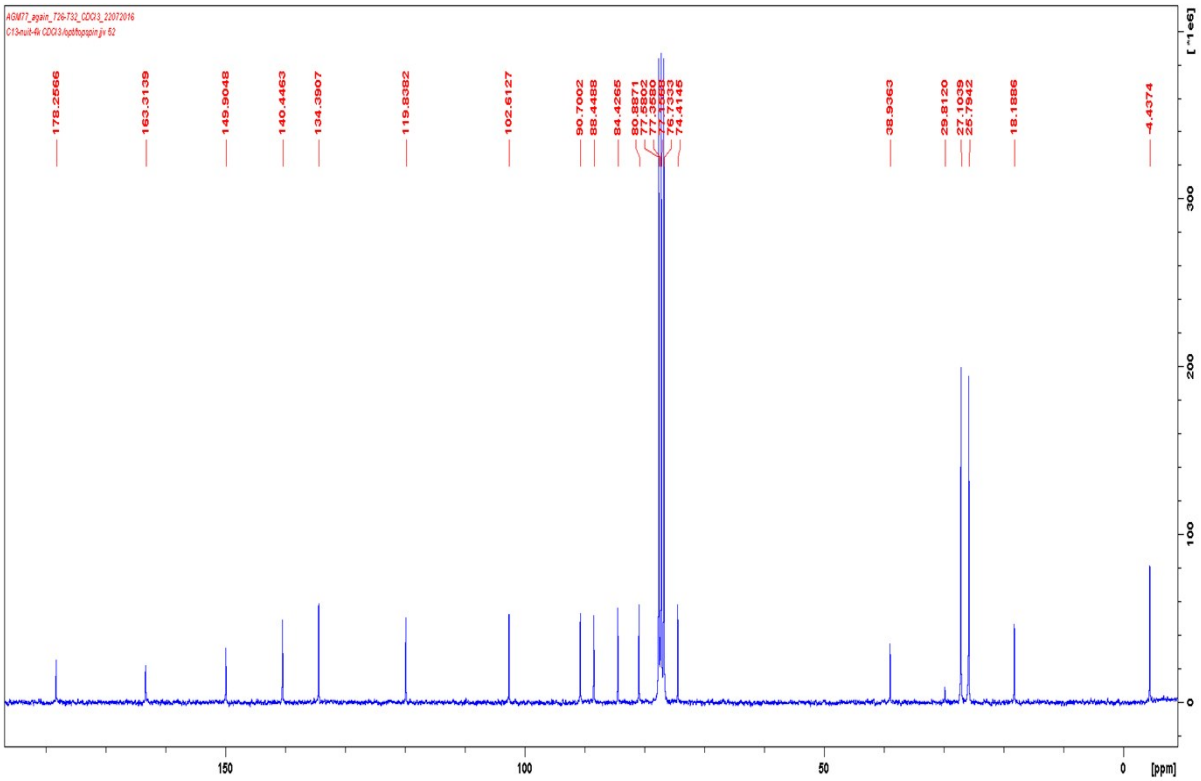

^{1}H NMR spectrum of **compound 5**

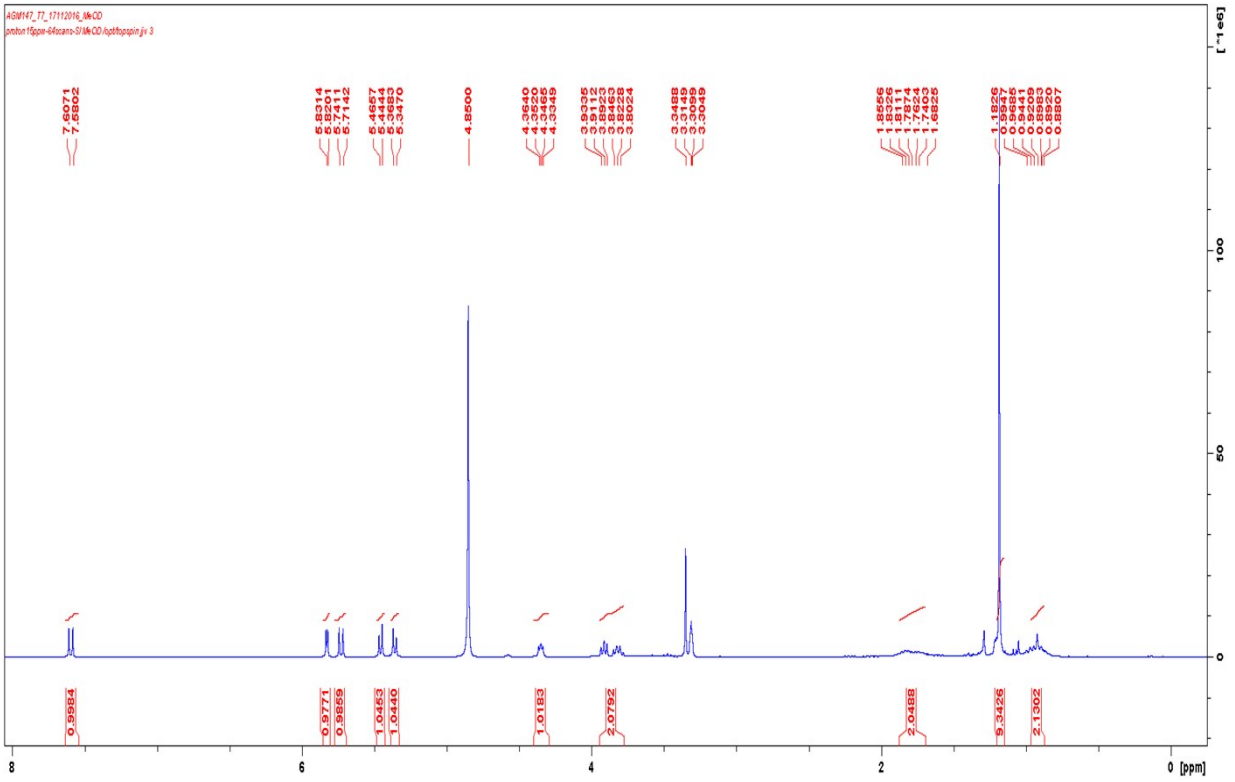

^{13}C NMR spectrum of **compound 5**

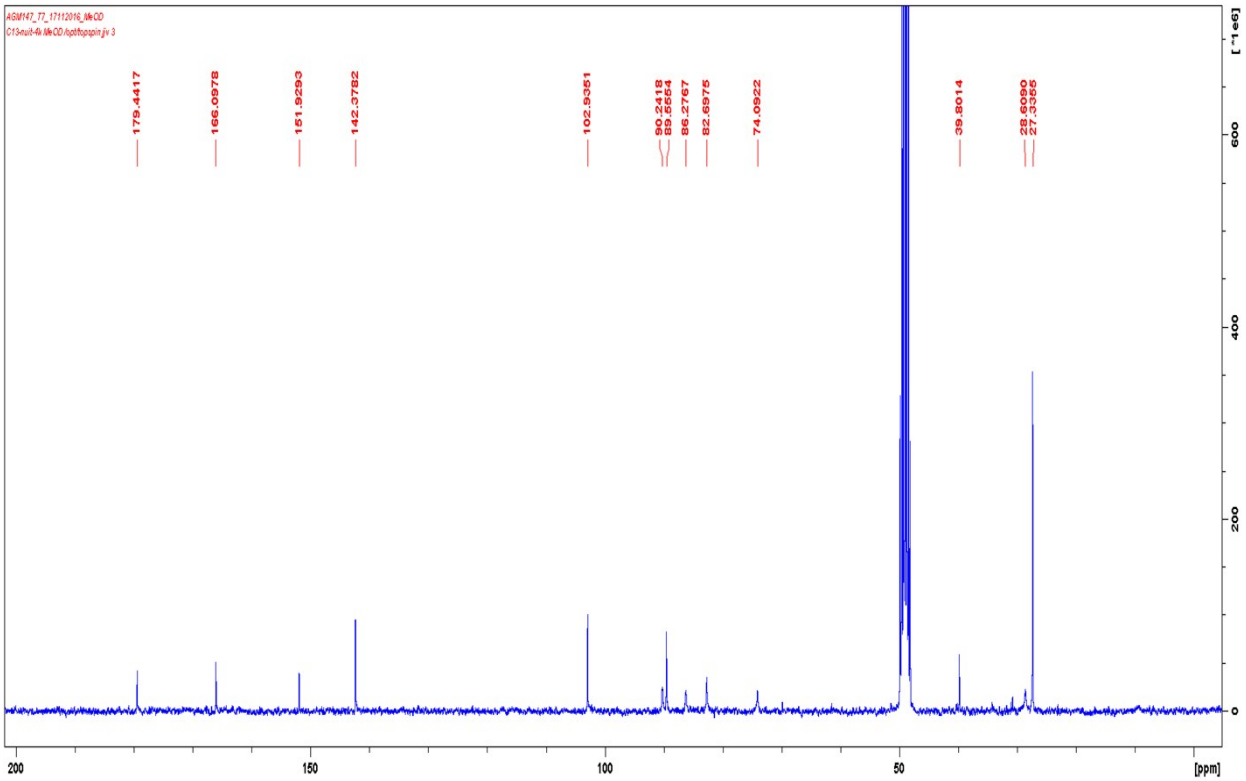

^{11}B NMR spectrum of **compound 5**

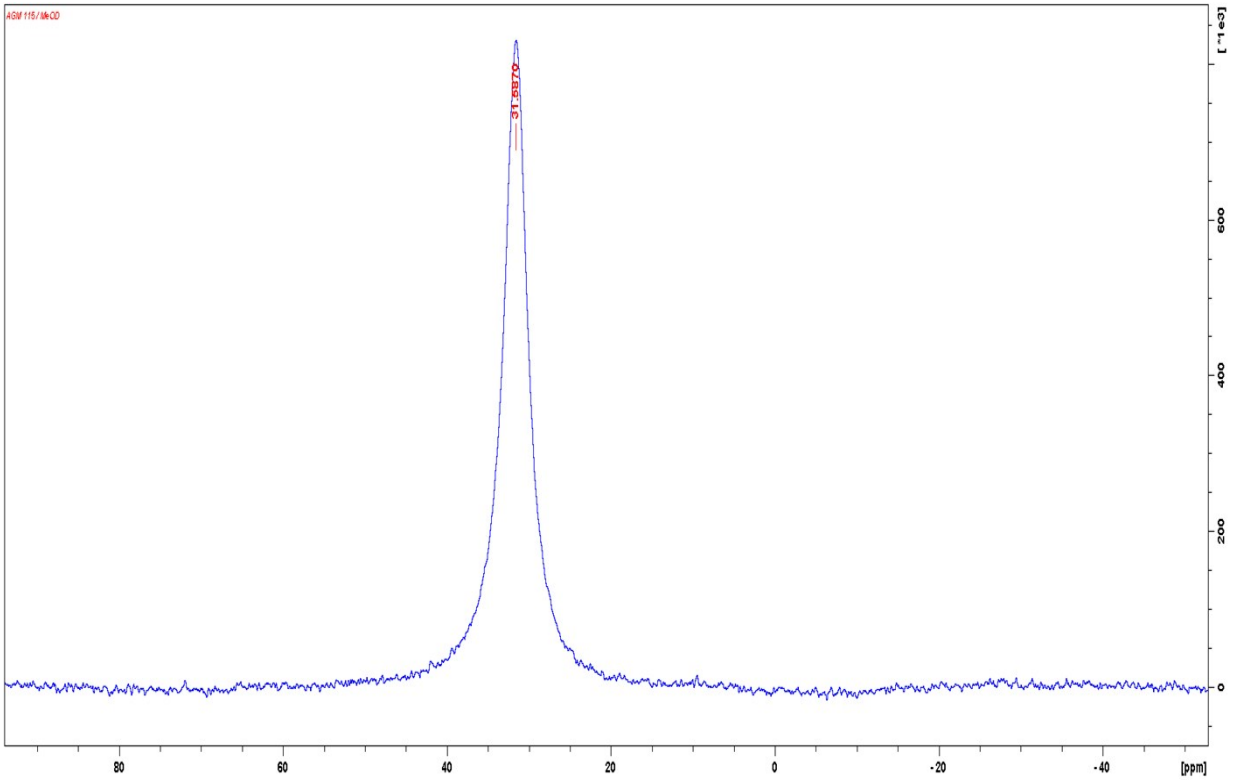

^{1}H NMR spectrum of **compound 6**

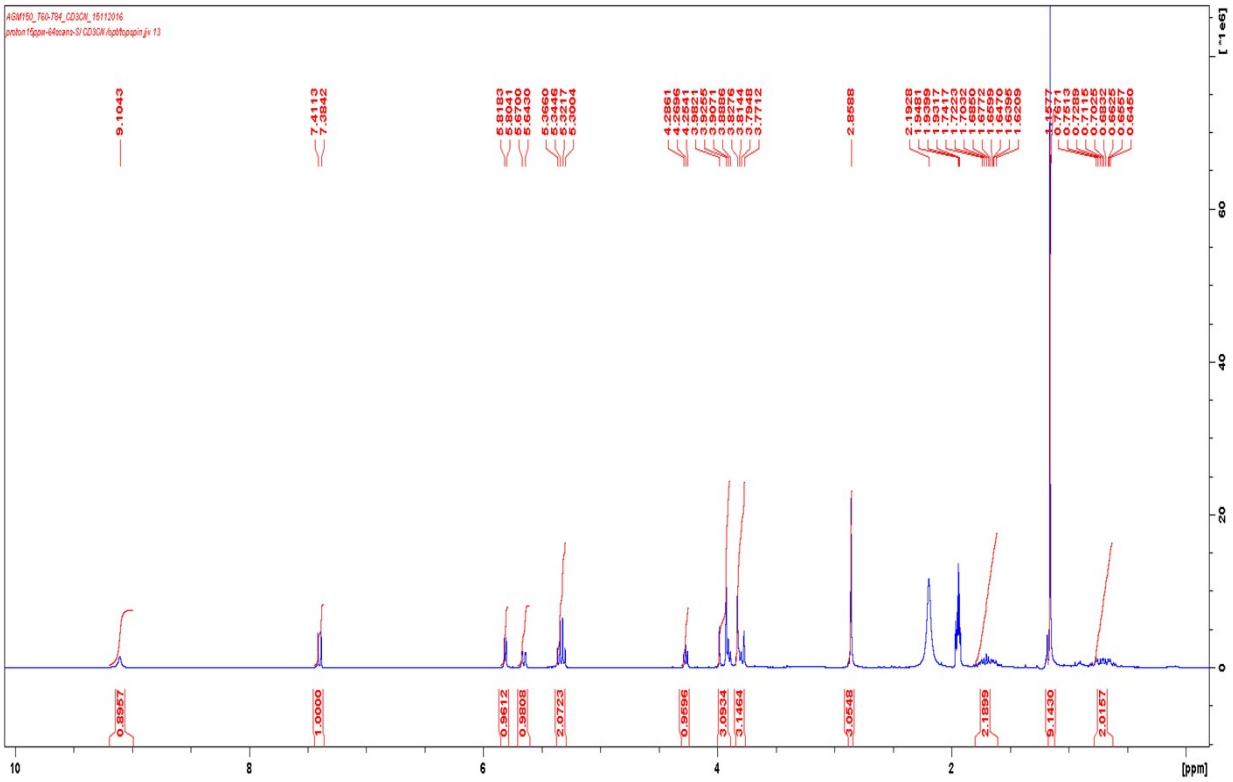

^{13}C NMR spectrum of **compound 6**

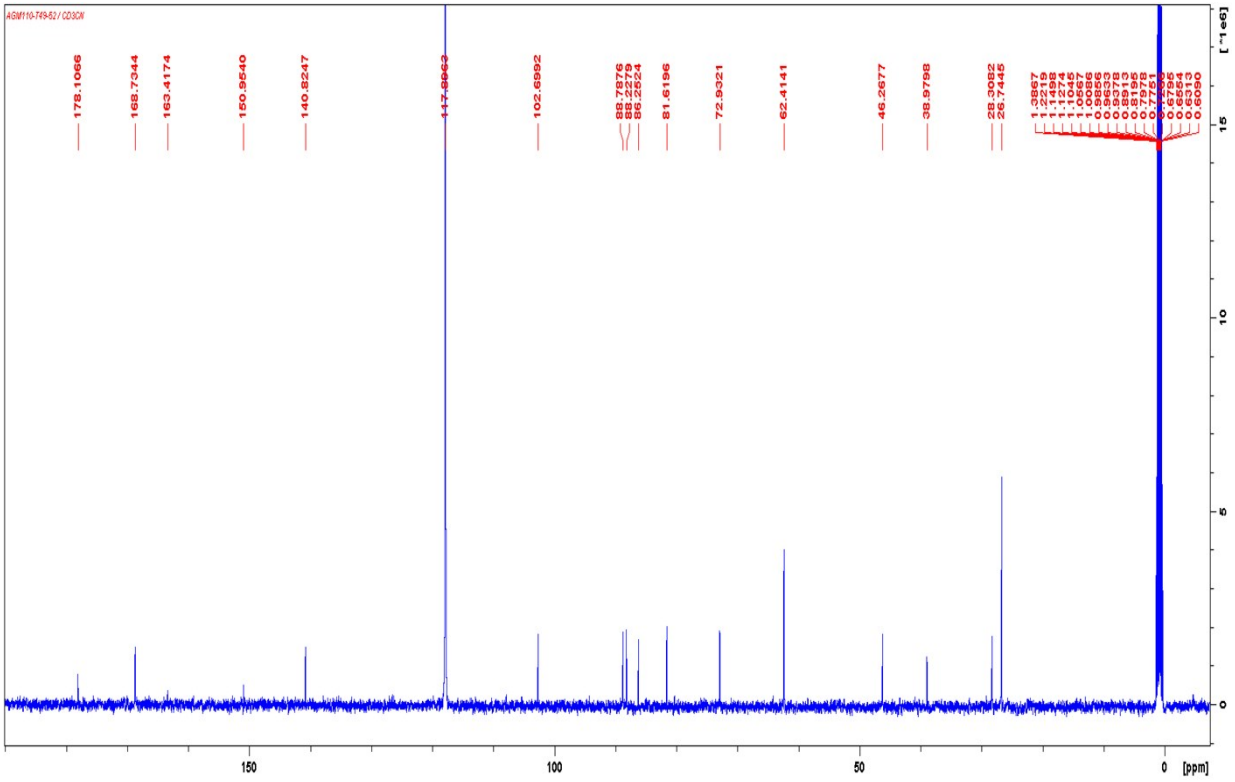

^{11}B NMR spectrum of **compound 6**

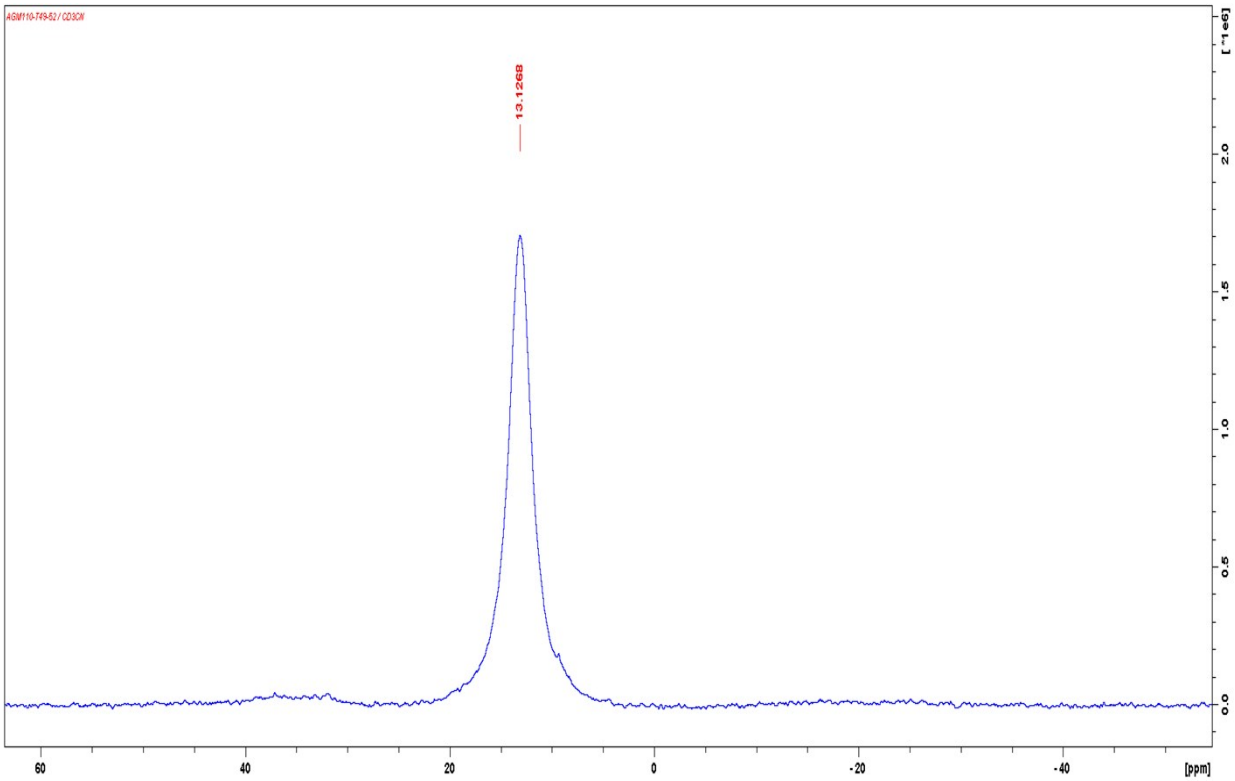

^{1}H NMR spectrum of **compound 7**

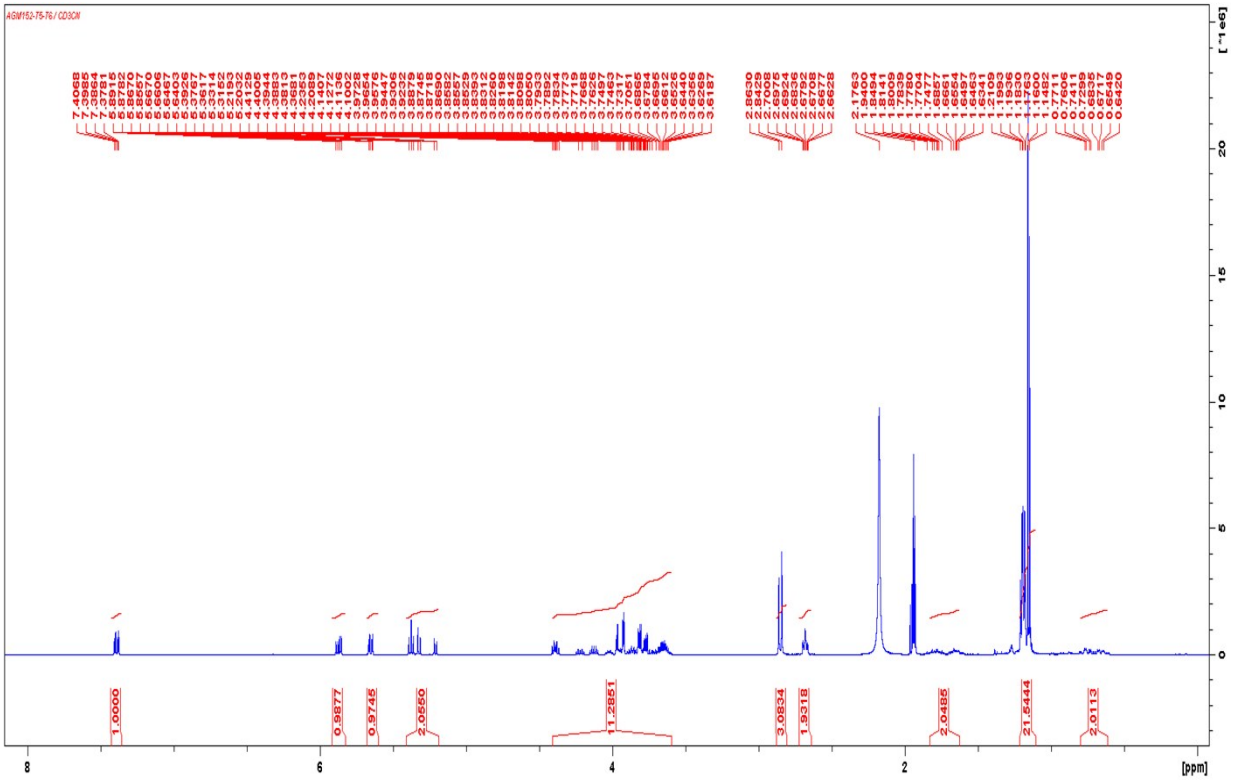

^{13}C NMR spectrum of **compound 7**

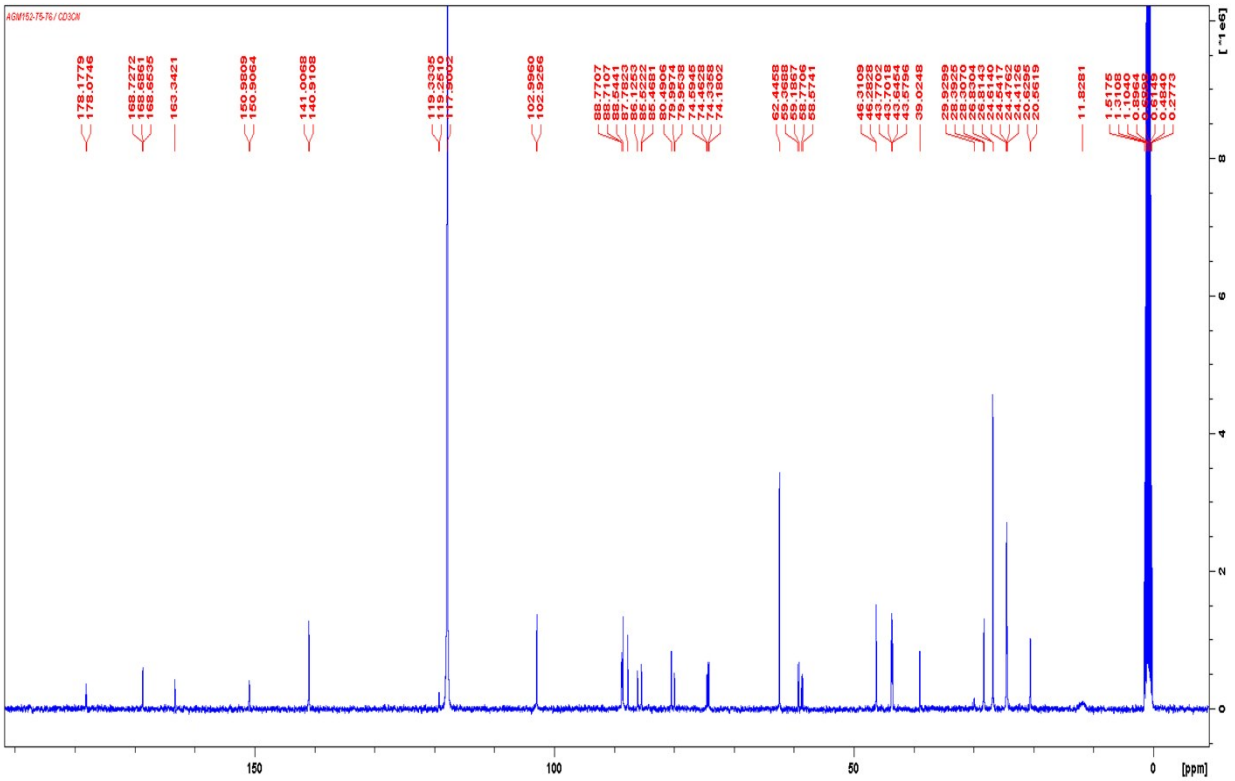

^{11}B NMR spectrum of **compound 7**

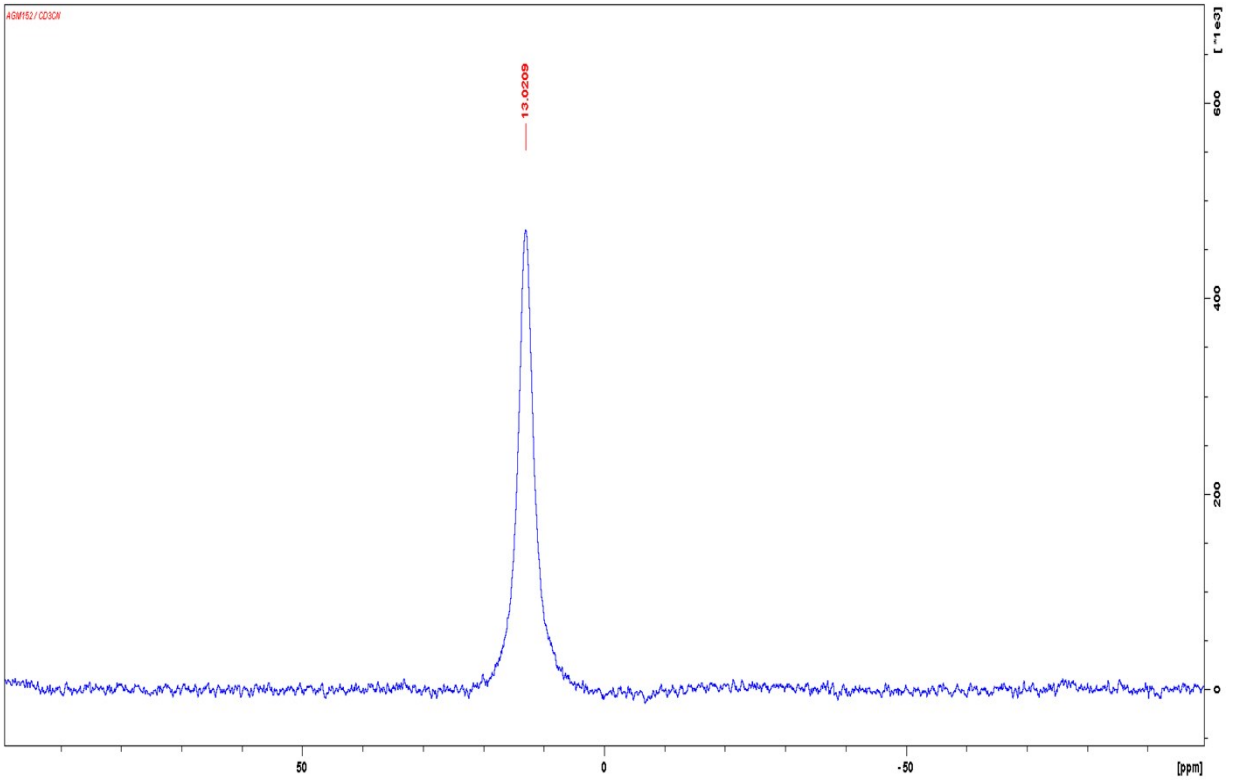

^{31}P NMR spectrum of **compound 7**

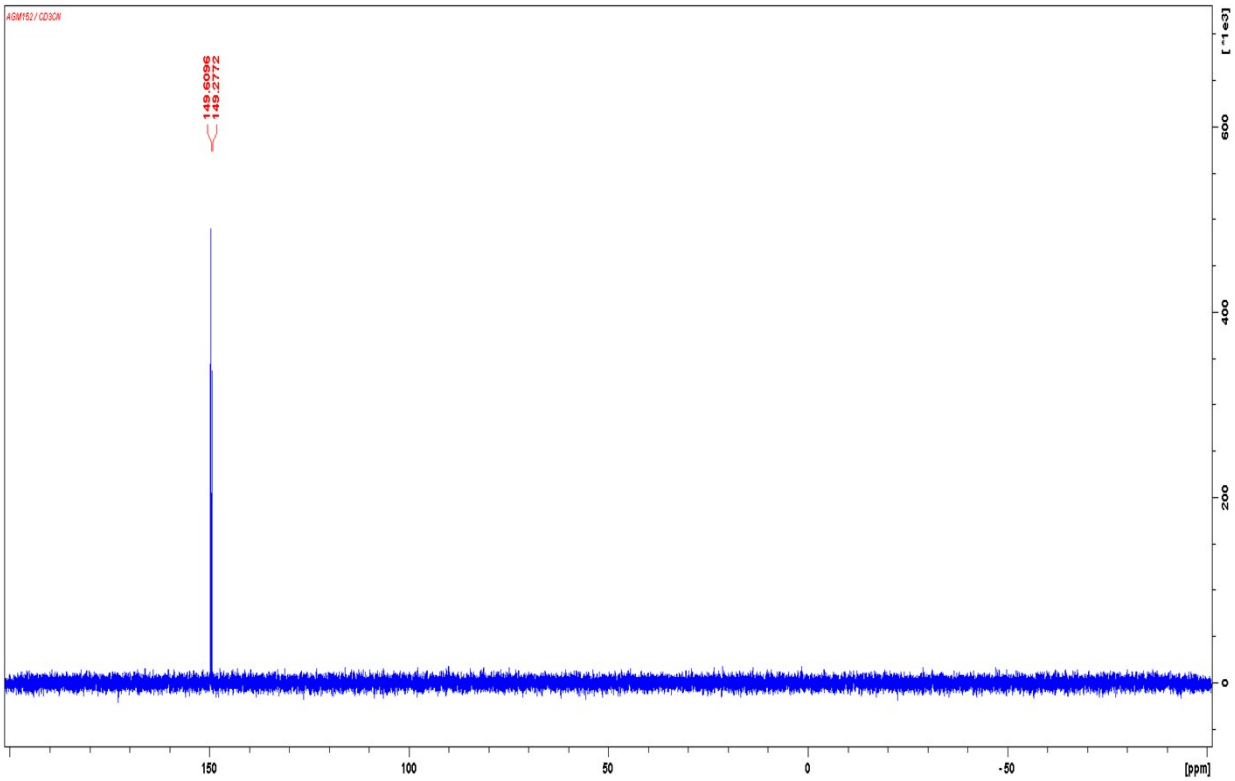

References

1. (a) D. Luvino, C. Baraguey, M. Smietana and J. J. Vasseur, *Chem. Commun.*, 2008, **44**, 2352; (b) A. R. Martin, I. Barvik, D. Luvino, M. Smietana and J.-J. Vasseur, *Angew. Chem., Int. Ed.*, 2011, **50**, 4193.
2. R. Barbeyron, J.-J. Vasseur and M. Smietana, *Chem. Sci.*, 2015, **6**, 542.
3. R. Barbeyron, A. R. Martin, J.-J. Vasseur and M. Smietana, *RSC Adv.*, 2015, **5**, 105587.
4. M. van Dijk and A. Bonvin, *Nucleic Acids Res.*, 2009, **37**, W235.
5. W. Humphrey, A. Dalke and K. Schulten, *Journal of Molecular Graphics & Modelling*, 1996, **14**, 33.
6. (a) K. Vanommeslaeghe, E. Hatcher, C. Acharya, S. Kundu, S. Zhong, J. Shim, E. Darian, O. Guvench, P. Lopes, I. Vorobyov and A. D. MacKerell, *J. Comput. Chem.*, 2010, **31**, 671; (b) K. Vanommeslaeghe and A. D. MacKerell, *Journal of Chemical Information and Modeling*, 2012, **52**, 3144; (c) K. Vanommeslaeghe and A. D. MacKerell, *Biochim. Biophys. Acta-Gen Subjects*, 2015, **1850**, 861; (d) K. Vanommeslaeghe, E. P. Raman and A. D. MacKerell, *Journal of Chemical Information and Modeling*, 2012, **52**, 3155.
7. W. L. Jorgensen, J. Chandrasekhar, J. D. Madura, R. W. Impey and M. L. Klein, *J. Chem. Phys.*, 1983, **79**, 926.
8. J. C. Phillips, R. Braun, W. Wang, J. Gumbart, E. Tajkhorshid, E. Villa, C. Chipot, R. D. Skeel, L. Kale and K. Schulten, *J. Comput. Chem.*, 2005, **26**, 1781.
9. T. E. Cheatham, J. L. Miller, T. Fox, T. A. Darden and P. A. Kollman, *J. Am. Chem. Soc.*, 1995, **117**, 4193.
10. J. P. Ryckaert, G. Ciccotti and H. J. C. Berendsen, *J. Comput. Phys.*, 1977, **23**, 327.